OUKA

**The University of Osaka
Institutional Knowledge Archive**

| Title	Contribution of germline and somatic mutations to risk of neuromyelitis optica spectrum disorder
Author(s)	Yata, Tomohiro; Sato, Go; Ogawa, Kotaro et al.
Citation	Cell Genomics. 2025, 5(3), p. 100776
Version Type	VoR
URL	https://hdl.handle.net/11094/100999
rights	This article is licensed under a Creative Commons Attribution-NonCommercial-NoDerivatives 4.0 International License.
Note	

The University of Osaka Institutional Knowledge Archive : OUKA

https://ir.library.osaka-u.ac.jp/

The University of Osaka

Contribution of germline and somatic mutations to risk of neuromyelitis optica spectrum disorder

Graphical abstract
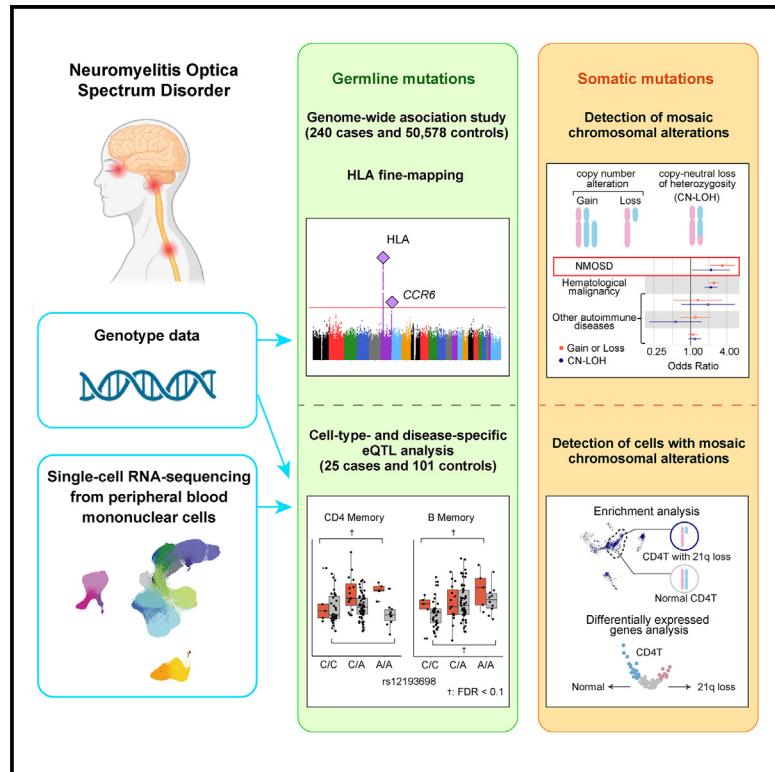
Authors

Tomohiro Yata, Go Sato,
Kotaro Ogawa, ..., Noriko Isobe,
Tatsusada Okuno, Yukinori Okada

Correspondence

isobe.noriko.342@m.kyushu-u.ac.jp
(N.I.),
okuno@neurol.med.osaka-u.ac.jp (T.O.),
yuki-okada@m.u-tokyo.ac.jp (Y.O.)

In brief

Yata et al. performed a genome-wide meta-analysis of neuromyelitis optica spectrum disorder (NMOSD) in Japanese individuals, identifying associations at the major histocompatibility complex region and *CCR6*. The *CCR6* risk variant showed a disease-specific expression quantitative trait loci effect in CD4T cell subsets. NMOSD was strongly associated with somatic mosaic chromosomal alterations. Single-cell analysis revealed that CD4T cells with 21q loss, one of the recurrently observed somatic events in NMOSD, showed dysregulation of type I interferon-related genes.

Highlights

- GWAS meta-analysis of NMOSD in Japanese identified associations at the MHC and *CCR6*

- The risk variant at *CCR6* showed disease-specific eQTL effects in CD4T cell subsets

- NMOSD was strongly associated with mCAs

- CD4T cells with 21q loss showed dysregulation of type I interferon-related genes

CellPress

Cell Genomics

CellPress
OPEN ACCESS

Article

Contribution of germline and somatic mutations to risk of neuromyelitis optica spectrum disorder

Tomohiro Yata,[1,2,3,45] Go Sato,[1,4,5,45] Kotaro Ogawa,[2,45] Tatsuhiko Naito,[1,5] Kyuto Sonehara,[1,5,6,7] Ryunosuke Saiki,[8] Ryuya Edahiro,[1,5,9] Shinichi Namba,[1,5,6] Mitsuru Watanabe,[10] Yuya Shirai,[1,9] Kenichi Yamamoto,[1,11,12] Ho NamKoong,[13] Tomoko Nakanishi,[5,6,14] Yuji Yamamoto,[1,9] Akiko Hosokawa,[2,15] Mamoru Yamamoto,[16] Japan MS/NMOSD biobank, The BioBank Japan Project, Japan COVID-19 Task Force, Eri Oguro-Igashira,[9,17] Takuro Nii,[9,18] Yuichi Maeda,[7,9,17] Kimiko Nakajima,[19] Rika Nishikawa,[20] Hiroaki Tanaka,[21] Shingo Nakayamada,[21] Koichi Matsuda,[22] Chikako Nishigori,[20] Shigetoshi Sano,[19] Makoto Kinoshita,[2] Ryuji Koike,[23] Akinori Kimura,[24] Seiya Imoto,[25] Satoru Miyano[26]

(Author list continued on next page)

[1]Department of Statistical Genetics, Osaka University Graduate School of Medicine, Suita, Japan
[2]Department of Neurology, Osaka University Graduate School of Medicine, Suita, Japan
[3]Department of Neurology, National Hospital Organization Osaka Toneyama Medical Center, Toyonaka, Japan
[4]Department of Gastroenterological Surgery, Osaka University Graduate School of Medicine, Suita, Japan
[5]Laboratory for Systems Genetics, RIKEN Center for Integrative Medical Sciences, Tsurumi, Japan
[6]Department of Genome Informatics, Graduate School of Medicine, The University of Tokyo, Tokyo, Japan
[7]Integrated Frontier Research for Medical Science Division, Institute for Open and Transdisciplinary Research Initiatives (OTRI), Osaka University, Suita, Japan
[8]Department of Pathology and Tumor Biology, Graduate School of Medicine, Kyoto University, Kyoto, Japan
[9]Department of Respiratory Medicine and Clinical Immunology, Osaka University Graduate School of Medicine, Suita, Japan
[10]Department of Neurology, Neurological Institute, Graduate School of Medical Sciences, Kyushu University, Fukuoka, Japan
[11]Department of Pediatrics, Osaka University Graduate School of Medicine, Suita, Japan
[12]Laboratory of Children's Health and Genetics, Division of Health Sciences, Osaka University Graduate School of Medicine, Suita, Japan
[13]Department of Infectious Diseases, Keio University School of Medicine, Tokyo, Japan
[14]Research Fellow, Japan Society for the Promotion of Science, Tokyo, Japan
[15]Department of Neurology, Suita Municipal Hospital, Suita, Japan
[16]Department of Neurology, Faculty of Medicine, University of Toyama, Toyama, Japan
[17]Laboratory of Immune Regulation, Department of Microbiology and Immunology, Osaka University Graduate School of Medicine, Suita, Japan

(Affiliations continued on next page)

SUMMARY

Neuromyelitis optica spectrum disorder (NMOSD) is a rare autoimmune disease characterized by optic neuritis and transverse myelitis, with an unclear genetic background. A genome-wide meta-analysis of NMOSD in Japanese individuals (240 patients and 50,578 controls) identified significant associations with the major histocompatibility complex region and a common variant close to *CCR6* (rs12193698; $p = 1.8 \times 10^{-8}$, odds ratio [OR] = 1.73). In single-cell RNA sequencing (scRNA-seq) analysis (25 patients and 101 controls), the *CCR6* risk variant showed disease-specific expression quantitative trait loci effects in CD4+ T (CD4T) cell subsets. Furthermore, we detected somatic mosaic chromosomal alterations (mCAs) in various autoimmune diseases and found that mCAs increase the risk of NMOSD (OR = 3.37 for copy number alteration). In scRNA-seq data, CD4T cells with 21q loss, a recurrently observed somatic event in NMOSD, showed dysregulation of type I interferon-related genes. Our integrated study identified novel germline and somatic mutations associated with NMOSD pathogenesis.

INTRODUCTION

Neuromyelitis optica spectrum disorder (NMOSD) is a rare autoimmune disease that primarily affects the central nervous system (CNS).[1] It is characterized by recurrent episodes of optic neuritis and longitudinally extensive transverse myelitis, typically causing devastating outcomes such as blindness and paralysis.[2] Anti-aquaporin 4 (AQP4) antibodies infiltrating the CNS play a pathogenic role and cause astrocyte damage in NMOSD.[3,4] The estimated prevalence of NMOSD is around 1 in 100,000 in Europe, while East Asian individuals have a higher prevalence, around 3.5 per 100,000.[5] This suggests that the ancestral background might affect the susceptibility of NMOSD.

Koichi Fukunaga,[27] Masahito Mihara,[28] Yuko Shimizu,[29,30] Izumi Kawachi,[31,32] Katsuichi Miyamoto,[33,34] Yoshiya Tanaka,[21] Atsushi Kumanogoh,[7,9,35,36] Masaaki Niino,[37] Yuji Nakatsuji,[16] Seishi Ogawa,[8,38,39] Takuya Matsushita,[10,40] Jun-ichi Kira,[10,41,42] Hideki Mochizuki,[2] Noriko Isobe,[10,*] Tatsusada Okuno,[2,*] Yukinori Okada[1,5,6,43,44,46,*]

[18]Department of Respiratory Medicine, National Hospital Organization Osaka Toneyama Medical Center, Toyonaka, Japan
[19]Department of Dermatology, Kochi Medical School, Kochi University, Nankoku, Japan
[20]Division of Dermatology, Department of Internal Related, Kobe University Graduate School of Medicine, Kobe, Japan
[21]The First Department of Internal Medicine, University of Occupational and Environmental Health, Kitakyushu, Japan
[22]Laboratory of Clinical Genome Sequencing, Graduate School of Frontier Sciences, The University of Tokyo, Tokyo, Japan
[23]Health Science Research and Development Center, Tokyo Medical and Dental University, Tokyo, Japan
[24]Institute of Research, Tokyo Medical and Dental University, Tokyo, Japan
[25]Division of Health Medical Intelligence, Human Genome Center, the Institute of Medical Science, the University of Tokyo, Tokyo, Japan
[26]M&D Data Science Center, Tokyo Medical and Dental University, Tokyo, Japan
[27]Division of Pulmonary Medicine, Department of Medicine, Keio University School of Medicine, Tokyo, Japan
[28]Department of Neurology, Kawasaki Medical School, Kurashiki, Japan
[29]Department of Neurology, Tokyo Women's Medical University, Tokyo, Japan
[30]Department of Medical Safety, Tokyo Women's Medical University, Tokyo, Japan
[31]Department of Neurology, Brain Research Institute, Niigata University, Niigata, Japan
[32]Medical Education Center, Graduate School of Medical and Dental Sciences, Niigata University, Niigata, Japan
[33]Department of Neurology, Kindai University School of Medicine, Osakasayama, Japan
[34]Department of Neurology, Wakayama Medical University, Wakayama, Japan
[35]Department of Immunopathology, Immunology Frontier Research Center (WPI-IFReC), Osaka University, Suita, Japan
[36]Center for Infectious Diseases for Education and Research (CiDER), Osaka University, Suita, Japan
[37]Department of Clinical Research, National Hospital Organization Hokkaido Medical Center, Sapporo, Japan
[38]Institute for the Advanced Study of Human Biology (WPI-ASHBi), Kyoto University, Kyoto, Japan
[39]Center for Hematology and Regenerative Medicine, Department of Medicine (MedH), Karolinska Institutet, Huddinge, Sweden
[40]Department of Neurology, Kochi Medical School, Kochi University, Nankoku, Japan
[41]Department of Neurology, Brain and Nerve Center, Fukuoka Central Hospital, Fukuoka, Japan
[42]Translational Neuroscience Center, Graduate School of Medicine, and School of Pharmacy at Fukuoka, International University of Health and Welfare, Fukuoka, Japan
[43]Laboratory of Statistical Immunology, Immunology Frontier Research Center (WPI-IFReC), Osaka University, Suita, Japan
[44]Premium Research Institute for Human Metaverse Medicine (WPI-PRIMe), Osaka University, Suita, Japan
[45]These authors contributed equally
[46]Lead contact
*Correspondence: isobe.noriko.342@m.kyushu-u.ac.jp (N.I.), okuno@neurol.med.osaka-u.ac.jp (T.O.), yuki-okada@m.u-tokyo.ac.jp (Y.O.)
https://doi.org/10.1016/j.xgen.2025.100776

To date, several genome-wide association studies (GWASs) have been conducted in NMOSD.[6–8] In Europeans, a meta-analysis of whole genome sequencing and genome-wide single-nucleotide polymorphism (SNP) array data revealed two independent signals associated with anti-AQP4 antibody-positive NMOSD in the major histocompatibility complex (MHC) region[7]; one of these signals was related to structural variants in the complement 4 (C4) region. In the same study, imputed human leukocyte antigen (HLA) data indicated a significant association between HLA-DRB1*03:01 and NMOSD. In the Japanese population, multiple HLA class II haplotypes, such as HLA-DRB1*08:02 and DRB1*09:01, have been reported to be associated with NMOSD.[8–10] Although a Japanese within-cases GWAS associated an intronic *KCNMA1* variant at 10q22 with disability score,[8] previous case-control GWASs did not detect any associations satisfying the genome-wide significance outside the MHC region.

Clonally expanded blood cells with somatic mutations, known as clonal hematopoiesis (CH), are common among peripheral blood of the general population[11,12] and increase the hematological cancer risks.[13,14] CH has increasingly been implicated in a variety of disease processes beyond malignancy[15,16] and gene-level mutations were associated with autoimmune diseases.[17] However, the potential impacts of mosaic chromosomal alterations (mCAs) on autoimmune diseases remain understudied. Furthermore, the biological insights into somatic mutations in benign (i.e., non-malignant) disorders have largely remained unexplored. Single-cell RNA sequencing (scRNA-seq) provides a unique opportunity to profile the mutational status of individual cells, enabling us to compare somatically mutated cells and their wild-type counterparts.[18,19] Integrating genomics and single-cell transcriptomics data should provide biological insights into the phenotypic effects of somatic mutations in non-malignant disorders.

In this study, we conducted a case-control GWAS meta-analysis of NMOSD in the Japanese population (240 NMOSD cases and 50,578 controls in total). We applied the HLA imputation method to the GWAS data to comprehensively fine-map the risk of the HLA variants. In scRNA-seq analysis, a novel risk variant of NMOSD outside the MHC region showed the disease-specific expression quantitative trait loci (eQTL) effects in subtypes of CD4$^+$ T (CD4T) cells. We further detected mCAs from the genotype data; our investigation including various autoimmune diseases provides the first evidence of the strong association between mCAs and the NMOSD risk. Projecting predefined mCAs into NMOSD scRNA-seq data, we demonstrated the cell-type-specific enrichment of mCAs and the expression change of immune-related genes in the somatically mutated cells. Our results demonstrated genetic contribution to this

Table 1. Genome-wide significant associations in the meta-analysis of NMOSD

Variant	Chr:Position	Gene	A1/A2	Discovery study				Replication study				Meta-analysis	
				AF		OR	P	AF		OR	P	OR	P
				Case	Control	(95% CI)		Case	Control	(95% CI)		(95% CI)	
All NMOSD (n = 240 cases, 50,578 controls)													
rs28383171	6:32,565,735	HLA-DRB1	C/T	0.21	0.39	0.41 (0.31–0.54)	4.6×10^{-11}	0.21	0.39	0.43 (0.29–0.63)	1.2×10^{-5}	0.41 (0.33–0.52)	1.0×10^{-14}
rs12193698	6:167,512,073	CCR6	C/A	0.49	0.35	1.8 (1.43–2.26)	2.7×10^{-7}	0.46	0.36	1.59 (1.13–2.26)	0.0043	1.73 (1.43–2.10)	1.8×10^{-8}
AQP4⁺ NMOSD (n = 223 cases, 50,578 controls)													
rs28383171	6:32,565,735	HLA-DRB1	C/T	0.19	0.39	0.36 (0.27–0.48)	1.4×10^{-12}	0.21	0.39	0.43 (0.28–0.65)	1.2×10^{-5}	0.38 (0.30–0.48)	9.6×10^{-16}
rs12193698	6:167,512,073	CCR6	C/A	0.49	0.35	1.79 (1.41–2.27)	7.1×10^{-7}	0.46	0.36	1.62 (1.12–2.33)	0.0048	1.74 (1.43–2.12)	4.9×10^{-8}

A1, reference allele; A2, alteration allele; AF, allele frequency of allele A2; AQP4⁺, anti-AQP4 antibody-positive; Chr, chromosome; CI, confidence interval; OR, odds ratio.

non-malignant yet deleterious disease across germline and somatic mutations.

RESULTS

Genome-wide association study of NMOSD in the Japanese population

In the discovery GWAS, we enrolled 163 NMOSD cases from the Japan MS/NMOSD biobank, and 40,908 controls from the BBJ Project[20] (Figures S1A and S1B; Table S1). After SNP imputation, we analyzed 8,707,965 autosomal variants and 261,946 X chromosome variants using a generalized linear mixed model. The most significant association signal that satisfied the genome-wide significance threshold of $p < 5.0 \times 10^{-8}$ was observed within the MHC region (rs28383171; $p = 4.6 \times 10^{-11}$, odds ratio [OR] = 0.41, 95% confidence interval [CI] 0.31–0.54; Table 1), which mapped 8,110 base pairs (bp) upstream of *HLA-DRB1*. To further explore the NMOSD risk SNPs, we conducted a replication GWAS that enrolled independent 77 NMOSD cases and 9,670 controls (Figures S1A and S1B; Table S1). Rs28383171 in the MHC region showed the strongest association in the replication GWAS ($p = 4.6 \times 10^{-5}$, OR = 0.43, 95% CI 0.29–0.63; Table 1).

After the meta-analysis combining the discovery and replication GWAS, we detected a novel risk variant at 6q27 outside the MHC region (rs12193698; $p = 1.8 \times 10^{-8}$, OR = 1.80, 95% CI 1.47–2.20; Figures 1A and S1B; Table 1), located 13 kbp upstream of the C-C motif chemokine receptor 6 (*CCR6*) gene (Figure 1B). CCR6 is a G protein-coupled receptor that binds C-C Motif Chemokine Ligand 20 (CCL20)[21] and is known as a cell surface marker of T helper 17 (Th17) cells.[22] Previous studies of animal models and of human subjects have reported associations of Th17 cells with the pathogenesis of NMOSD.[23–25] In anti-AQP4 antibody-positive patients (n = 223), the same variant also exhibited a significant association ($p = 4.9 \times 10^{-8}$, OR = 1.74, 95% CI 1.43–2.12; Table 1). Previous European NMOSD GWAS[7] showed no association signals around this variant (Table S2). Thus, our genetic study demonstrated a novel Japanese population-specific locus.

NMOSD shares a genetic background with other autoimmune diseases

Previous GWASs of immune-related diseases, such as rheumatoid arthritis (RA) and primary biliary cholangitis (PBC), showed a strong association with *CCR6*.[26–28] Clinically, NMOSD coexists with other autoimmune diseases,[29–31] but its etiology is unclear. To investigate the genetic correlation, we compared the results of our NMOSD GWAS with those of autoimmune diseases in East Asian individuals.

First, we examined the previous studies of RA[27] and PBC[28] as *CCR6*-associated diseases. The effects of risk variants in these two diseases were significantly correlated with NMOSD ($p = 0.0073$, Spearman's $\rho = 0.53$ for RA; $p = 4.0 \times 10^{-4}$, Spearman's $\rho = 0.85$ for PBC; Figures S2A and S2B; Table S3). We additionally examined systemic lupus erythematosus (SLE),[32] which frequently coexists with NMOSD. The 94 of 111 SLE risk variants outside the MHC region were available in our NMOSD study, and their effect sizes showed significantly positive correlations between SLE and NMOSD ($p = 1.1 \times 10^{-10}$, Spearman's
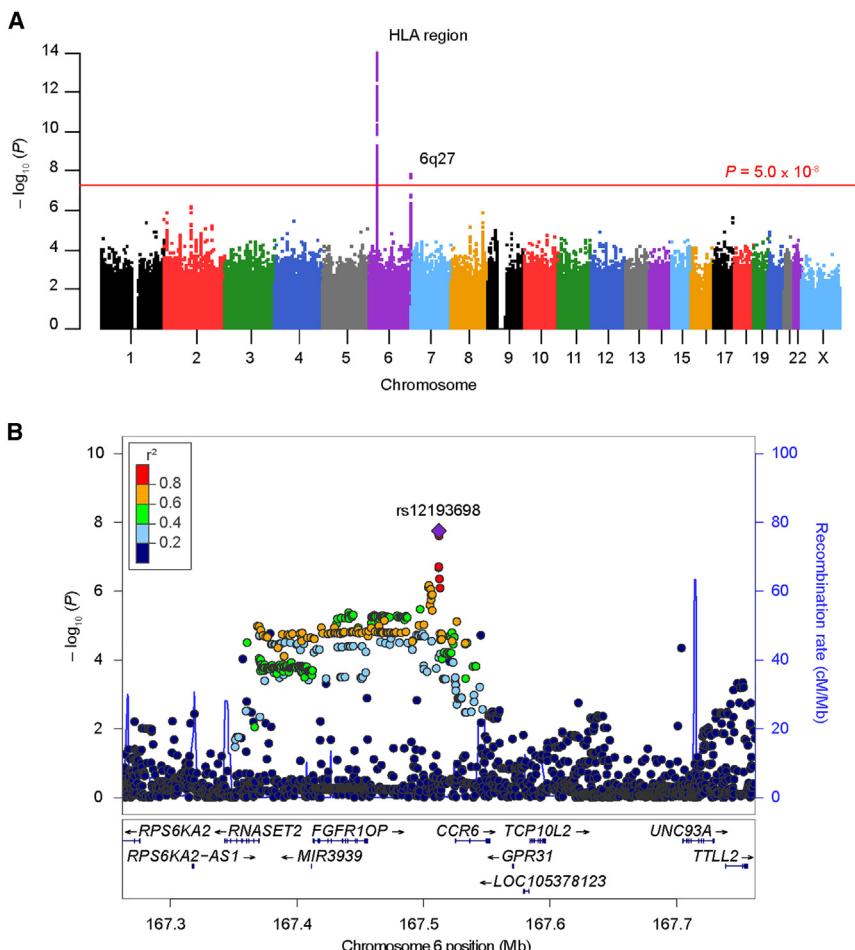
Figure 1. NMOSD GWAS meta-analysis of Japanese individuals

(A) Manhattan plot of the NMOSD GWAS meta-analysis. The red horizontal line indicates the genome-wide significance threshold of $p = 5.0 \times 10^{-8}$.

(B) Regional association plot around the lead variant, rs12193698, at *CCR6*. The purple diamond indicates the lead variant, rs12193698. Other dots represent SNPs and are colored according to linkage disequilibrium (r^2) with the lead variant.

$\rho = 0.60$; Figure S2C; Table S3). Especially, a variant within *STAT4* (rs11889341) was significantly associated with RA, PBC, and SLE; it also showed a nominal association with NMOSD. These findings indicate that these autoimmune diseases have shared genetic backgrounds.

Associations of the HLA with NMOSD susceptibility

We then focused on the association signal within the MHC region. To fine-map the causal HLA variants, we applied HLA imputation to GWAS meta-analysis data and performed MHC fine-mapping for the NMOSD susceptibility. We found the strongest association at HLA-DRβ1 amino acid position 11 ($p = 3.7 \times 10^{-17}$; Figure 2A; Table 2). Given the strength and complexity of the association within the region covering HLA-DRB1, -DQB1, and -DQA1, we performed conditional analysis within this region to identify independent associations. When conditioning on HLA-DRβ1 amino acid position 11, we identified the most significant independent association in HLA-DQB1*06 ($p = 7.6 \times 10^{-10}$; Figure 2B; Table S4). We observed non-additive effects of amino acid polymorphisms of HLA-DRβ1 amino acid position 11 and HLA-DQB1*06 on the NMOSD susceptibility, particularly HLA-DRβ1 Ser11 ($p = 3.3 \times 10^{-4}$; Table S5). When conditioning on HLA-DRβ1 amino acid position 11 and HLA-DQB1*06, we did not observe any additional independent association in *HLA-DRB1*, *-DQA1*, and *-DQB1* ($p > 0.05$; Figure 2B; Table S4). When conditioning on *HLA-DRB1*, *-DQA1*, and *-DQB1*, we did not observe any significant association ($p > 0.05$; Figure 2A). We performed fine-mapping for anti-AQP4 antibody-positive patients and the same variant, HLA-DRβ1 amino acid position 11, exhibited the most significant association ($p = 1.1 \times 10^{-18}$; Figure S3; Table 2).

***CCR6* expression profile in scRNA-seq data**

GWASs identified the NMOSD-associated variant in the *CCR6* locus. We therefore sought to reveal the functional role of *CCR6* in NMOSD. To elucidate the cell-type-specific expression profile of *CCR6*, we performed scRNA-seq in peripheral blood mononuclear cells (PBMCs) from 25 NMOSD patients and 101 healthy controls (Table S6). After processing the samples through the unified single-cell analysis pipeline, we obtained 1,004,361 immune cells. We manually annotated cells based on the expression of known marker genes,[33] which led to the definition of seven major cell types and 19 more detailed subsets (Figures 3A, S4, and S5; Table S7). Among the 19 detailed cell types, we found enrichment of *CCR6* expression in CD4^{+} memory T (CD4 memory) cells, regulatory T (Treg) cells, mucosal-associated invariant T (MAIT) cells, naive B (B naive) cells, and memory B (B memory) cells (Figures 3B and 3C). This expression profile was consistent with previous reports.[21,34] Case-control differential expression analysis in these five cell types revealed the significant upregulation of *CCR6* expression level in CD4 memory and MAIT cells in NMOSD (false discovery rate [FDR] = 2.1×10^{-4}, $\log_2$ fold change [FC] = 0.57 for CD4 memory; FDR = 0.0048, $\log_2$ FC = 0.52 for MAIT; Table S8), implying that *CCR6* is important in T cell subtypes in the context of NMOSD.

Cell-type- and disease-specific eQTL effects of the NMOSD-related variant

To examine the regulation of the transcriptional variability and dynamics of *CCR6* by the GWAS risk variant (rs12193698), we performed eQTL analyses, separately for NMOSD cases and healthy
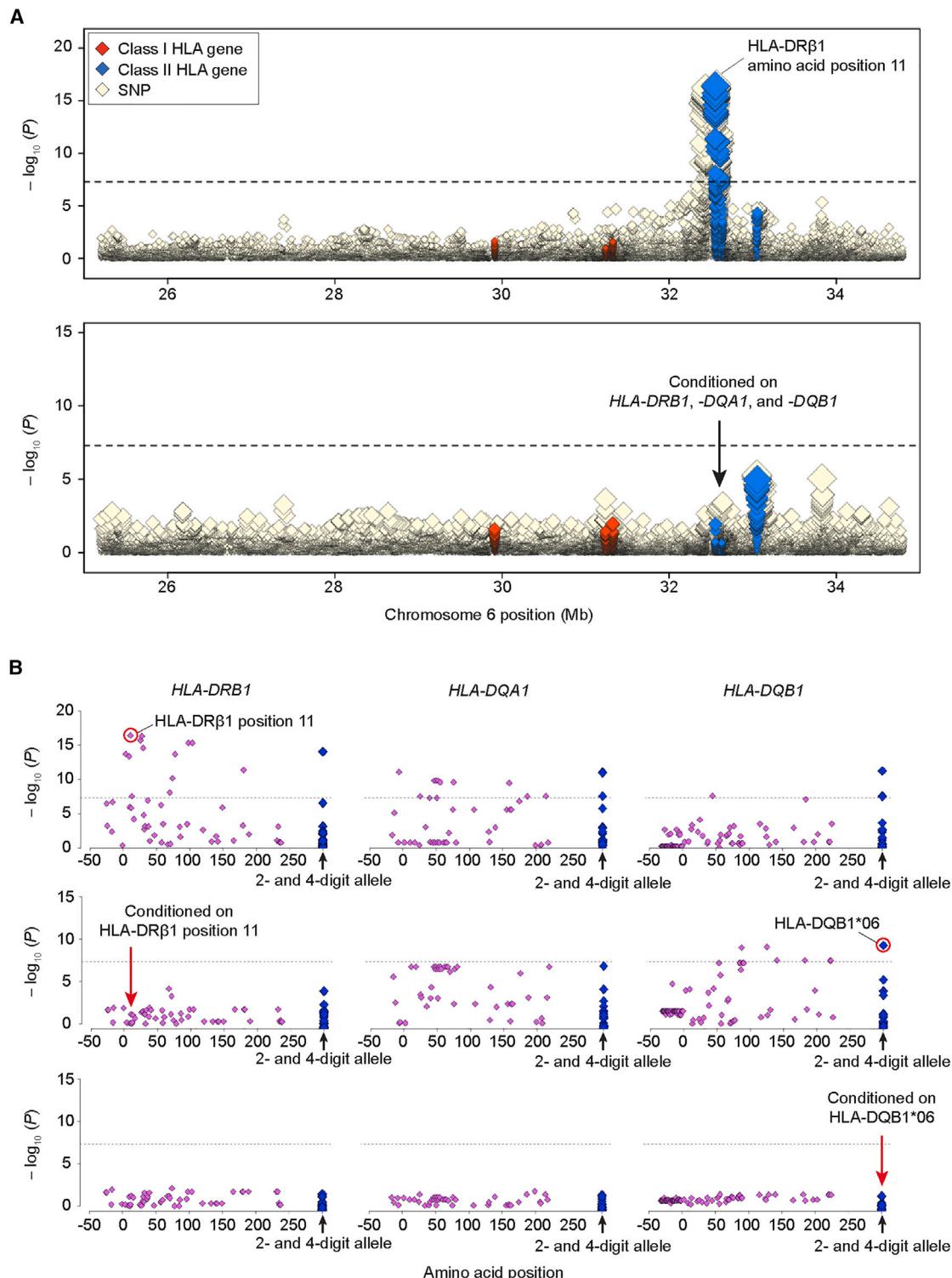
Figure 2. Regional association plots of HLA variants with NMOSD risk NMOSD GWAS meta-analysis of Japanese individuals

(A) Regional association plots in nominal results (upper) and those conditioned on *HLA-DRB1*, *-DQA1,* and *-DQB1* (lower). In each plot, diamonds represent the HLA variants, including SNPs, classical alleles, and amino acid polymorphisms of the tested HLA genes. The dashed horizontal lines represent the genome-wide significance threshold of $p = 5.0 \times 10^{-8}$.

controls. In MAIT, B naive, and B memory cells, both NMOSD and control cohorts showed significant eQTL effects of the risk variant on *CCR6* expression levels (FDR <0.1). By contrast, the risk variant showed NMOSD-specific increasing dosage effects in CD4 memory (FDR = 0.069, β = 0.037 for NMOSD; FDR = 0.89, β = 0.0011 for controls) and Treg cells (FDR = 0.069, β = 0.040 for NMOSD; FDR = 0.89, β = 0.0034 for controls; Figure 3D; Table S9). The previous study using bulk RNA-seq data showed generally consistent eQTL effect in immune cells with our control cohort (Figure S6). In our study, the NMOSD cohort showed higher eQTL effects than controls, particularly in T cell subtypes: CD4 memory, Treg, and MAIT cells (Figure 3E). These results demonstrated that the risk allele of rs12193698 might contribute to the pathogenesis of NMOSD by upregulating *CCR6* in T cell subtypes, especially in CD4T subsets. To further explore the role of CD4T cells in NMOSD, we performed cell-cell interaction analysis between CD4T cells and other cell types. We inferred intercellular communications by the expression of ligand-receptor pairs using CellChat.[35] Ligand-receptor communications from CD4 naive and CD4 memory cells to CD8 memory and CD8 CTL cells were enhanced in NMOSD patients (Figure S7A). Focusing on *CCL20/CCR6* interaction, CD4 memory cells (receivers) showed the strong interaction with mono CD14 cells (senders), which was enhanced in the context of NMOSD (Figure S7B). Taken together, CD4 memory cells play a specific role in NMOSD.

The contribution of Th17 cells to NMOSD

Given that our analysis revealed the significant impact of CD4 memory cells, we attempted to extract Th17 cells, a subset of CD4T cells playing a crucial role in the pathogenesis of NMOSD.[23–25] To perform the more detailed immune cell annotation, we projected CD4T cells of our scRNA-seq data onto a previous dataset of CD4T subsets including Th17 cells[36] (Figures 4A–4C). Most of the Th17 cells annotated based on the reference data were included in the CD4 memory cells in our dataset and highly expressed *CCR6* compared with other CD4T cells (Figures 4D and 4E). In the differential abundance analysis, the proportion of non-naive CD4T cells, including Th17 cells, was increased in NMOSD (Figure 4F). In the differential expression analysis of Th17 cells, *CCR6* was significantly upregulated in NMOSD (Table S8). We analyzed the aforementioned eQTL effect on CD4 memory cells separately for Th17 cells and other cells. Although the limited number of cells resulted in reduced statistical power, eQTL effects were relatively higher in Th17 cells compared with other CD4 memory cells (Figure 4G; Table S9). We confirmed that Th17 cells play a significant role in the pathogenesis of NMOSD.

Effects of the NMOSD-related variant on plasma protein levels

In addition to eQTL analysis, we performed plasma protein quantitative trait loci (pQTL) analysis to examine the effect of GWAS

risk variant (rs12193698) on the concentration of plasma proteins. We measured expression levels of 2,943 proteins using Olink Explore 3072 platform from 1,394 independent Japanese.[37–39] CCR6 was not included in this dataset. We found a significant pQTL effect of rs12193698 only on ribonuclease T2 (RNase T2) and risk alleles reduced the expression level (Figures S8A and S8B). RNase T2 is an endoribonuclease that degrades exogenous RNA molecules into forms detected by toll-like receptor 8 (TLR8).[40] Downstream of TLR8 includes transcription factors such as NF-κB and IRF3 that affect CD4T cell differentiation.[41] The previous study has reported that downregulation of TLR8 may contribute to autoimmune processes in multiple sclerosis (MS).[42] Decreased expression of RNase T2 may also affect the pathogenesis of NMOSD by dysregulating the TLR8 pathway.

Mosaic chromosomal alterations increase the NMOSD risk

As described above, we have so far analyzed the effect of the germline mutation on NMOSD. To further expand our NMOSD risk catalog, we then investigated the association between somatically acquired mCAs and the risk of NMOSD. The MoChA pipeline[11,12] was applied to the GWAS data from patients with various autoimmune diseases: RA, MS, SLE, psoriasis vulgaris, Sjögren's syndrome, sarcoidosis (median n_{Case} = 287), or hematological malignancy (n = 1,301) and control subjects (n = 48,394; Table S10), identifying individuals with autosomal mCAs including gain, loss, and copy-neutral loss of heterozygosity (CN-LOH). We evaluated the associations between each disease and copy number alteration (CNA; gain or loss) or CN-LOH using a multivariate logistic regression analysis adjusted for age and sex (Figure 5A). As expected,[13,14] hematological malignancy showed strong associations with CNA (OR = 2.43, 95% CI 2.03–2.92) and CN-LOH (OR = 2.17, 95% CI 1.71–2.76). Among the autoimmune diseases, only NMOSD was associated with CNA at extremely high OR (OR = 3.37, 95% CI 2.10–5.41) and CN-LOH (OR = 2.18, 95% CI 1.07–4.46). Thus, we propose that mCAs increase the risk of NMOSD, perhaps more strongly than that of hematological malignancy.

Dissection of somatically mutated cells in NMOSD patients at single-cell resolution

To reveal the biological mechanisms underlying the association between mCAs and NMOSD, we additionally conducted scRNA-seq of four NMOSD patients with mCAs detected using the GWAS genotype data (mNMOSD1-4; Figure 5B; Table S11). In the genotype data, three NMOSD patients (mNMOSD1-3) showed mCAs at 21q, which was one of the recurrently affected regions in NMOSD patients and did not show an association with hematological malignancy (i.e., NMOSD-specific; Figure S9A; Table S12). We used Numbat[43] to distinguish the somatically mutated cells from the other normal cells at single-cell resolution. As Numbat uses germline allelic signals from scRNA-seq raw reads for

---

(B) Association plots in *HLA-DRB1*, -*DQA1*, and -*DQB1* genes. Diamonds represent the amino acid polymorphisms (purple) and classical alleles (blue) for the tested HLA genes. For amino acid polymorphisms, the smallest *p* values among those for results of binary and omnibus tests at each position are shown. An allele or position of the smallest *p* values at each step is displayed in a red circle. The dashed horizontal lines represent the genome-wide significance threshold of *p* = 5.0×10^{-8}.

Table 2. Nominal associations of HLA-DRβ1 amino acid position 11 with NMOSD

		All NMOSD				AQP4+ NMOSD			
		Frequency				Frequency			
		Case	Control	OR (95% CI)	P	Case	Control	OR (95% CI)	P
HLA-DRβ1 amino acid position 11	Omunibus test	–	–	–	3.7×10^{-17}	–	–	–	1.1×10^{-18}
	Aspartic acid	0.040	0.15	0.24 (0.15–0.37)	9.3×10^{-15}	0.034	0.15	0.20 (0.12–0.33)	1.2×10^{-15}
	Leucine	0.088	0.057	1.57 (1.15–2.16)	0.0083	0.087	0.057	1.57 (1.13–2.18)	0.011
	Proline	0.21	0.19	1.19 (0.95–1.48)	0.13	0.22	0.19	1.20 (0.96–1.51)	0.12
	Serine	0.48	0.37	1.56 (1.31–1.87)	1.4×10^{-6}	0.49	0.37	1.64 (1.36–1.98)	2.4×10^{-7}
	Valine	0.18	0.23	0.71 (0.56–0.89)	0.0025	0.17	0.23	0.66 (0.52–0.85)	7.5×10^{-4}

AQP4+, anti-AQP4 antibody-positive; CI, confidence interval; OR, odds ratio.

somatic clone detection, we expected that more detailed allele information in scRNA-seq data would achieve more sensitive detection. For the additional scRNA-seq, we applied a long and deep sequencing method increasing a target depth from 20,000 to 80,000 reads per cell and extending a read2 length from 90 to 270 bp. Consequently, we could identify somatically mutated cells for the four NMOSD patients (Figures 5C and S9B).

All the mCA events were found to be highly cell-type-specific and the somatic mutations at 21q were enriched in T lymphocytes (Figures 5D and 5E; Table S13). Notably, the two NMOSD patients with 21q loss consistently showed enrichment of the mutated cells in CD4T cells (mNMOSD1: OR = 2.2 for CD4T; mNMOSD2: OR = 2.4 for CD4T). This suggests that not only germline variations, but somatic mutations have the phenotypic impacts on CD4T cells in NMOSD. In CD4T cells, CD4 memory and Treg cells showed relatively high fractions of the mutated cells in mNMOSD1 and mNMOSD2, respectively (Figure S9C). To assess the correlation between these somatically mutated clones and T cell receptor (TCR) clonotypes, we integrated scRNA-seq and scVDJ-seq data. While the 21q loss clones were expanded independently of the TCR repertoire, we observed a large TCR clonotype (clone size = 315 [mean clone size = 3.6]) consisting of more than 70% mutated cells with 21q gain in mNMOSD3, implying different underlying mechanisms among 21q loss and 21q gain (Figure S9D).

To evaluate the phenotypic impacts of 21q loss in mNMOSD1 and mNMOSD2, we assessed differentially expressed genes (DEGs) between the mutant and normal CD4T cells (Figure 4F; Table S14). Most of the top downregulated genes in the 21q loss CD4T cells were located in the affected chromosomal region, highlighting the successful detection of the mutant clones. We performed a pathway enrichment analysis and found that the downregulated DEGs in CD4T cells with 21q loss were enriched in type I interferon (IFN-I)-related pathways (Figures 5G and S10). The somatic mutation might suppress the expressions of interferon receptor genes residing within 21q (i.e., cis; IFNAR1 and IFNAR2), resulting in downregulation of IFN-related genes outside the affected regions (i.e., trans; OAS1 and STAT2). Given that a fraction of NMOSD patients showed mCAs at 21q, our results may highlight the significance of IFN-I signaling in the NMOSD pathophysiology. We dissected the somatically mutated cells with an NMO-specific mCA at single-cell resolution and demonstrated the potential mechanisms underlying the strong association between mCAs and the NMOSD risk.

DISCUSSION

In this study, we obtained new insights into the pathogenesis of NMOSD from two aspects: germline and somatic mutations. By combining scRNA-seq data in both approaches, we confirmed cell-type-specific effects, especially in CD4T cells.

Our GWAS meta-analysis identified NMOSD risks at the MHC region and CCR6, a novel associated gene. We further performed HLA fine-mapping analysis and found that HLA-DRβ1 amino acid position 11 and HLA-DQB1*06 were associated with the NMOSD susceptibility. A previous European study also showed significant associations of class II HLA variants.[7] Although the same study identified the association of the structural variation in the C4 region, our study showed no associations around this region. This result might be due to the HLA diversity among populations, thus genetic studies including multiple populations are warranted. CCR6 is highly expressed in Th17 cells,[21,22] and plays an important role in the pathogenesis of autoimmune diseases. Our study revealed the shared genetic backgrounds of NMOSD with RA, PBC, and SLE. The proportion of Th17 cells and the levels of Th17-related cytokines have been reported to increase in NMOSD patients,[24,25] and we also confirmed a high abundance of Th17 cells in our dataset. Some studies have shown that CCL20/CCR6 interaction promotes the migration of Th17 cells, disruption of the blood-brain barrier, and invasion of inflammatory cells into the CNS.[44,45] The increased CCL20/CCR6 interaction between CD4 memory cells and monocytes in our NMOSD dataset suggests an enhanced inflammatory reaction leading to CNS damage.[46] We identified the disease-specific eQTL effects of the NMOSD risk variant in CD4 memory and Treg cells. Notably, Th17 cells within the CD4 memory subset exhibited relatively larger eQTL effects. The cell-type-specific eQTL analysis enabled us to functionally interpret the GWAS result and demonstrated genetic regulation underlying the pathogenic role of Th17 cells in NMOSD.

CH including mCAs and gene-level mutations has increasingly been found to contribute to various disease processes beyond malignancy.[15,16] As the mCA detection method typically utilizes genotype data from large-scale cohorts such as biobanks, previous efforts mainly focused on common diseases such as
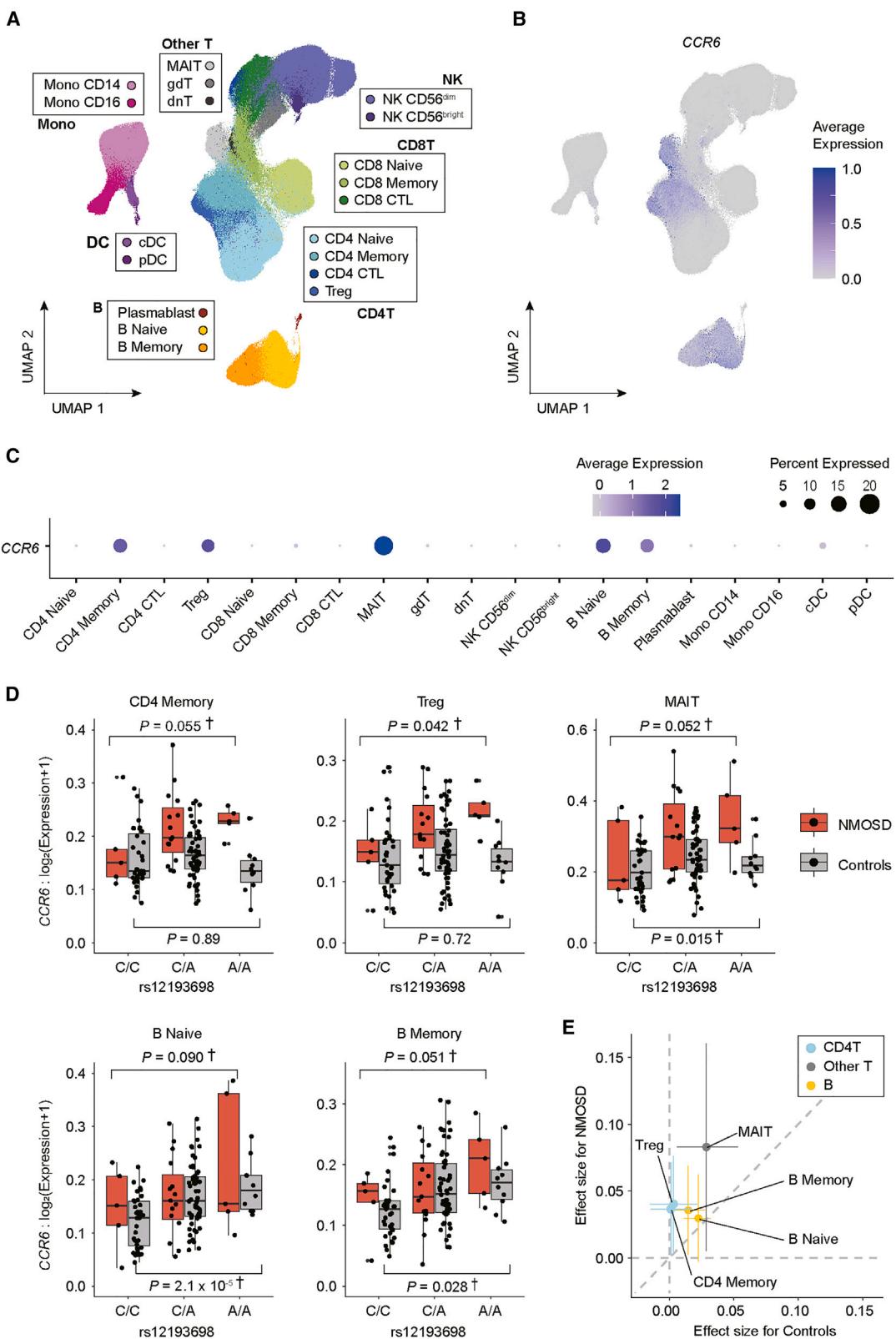
(legend on next page)
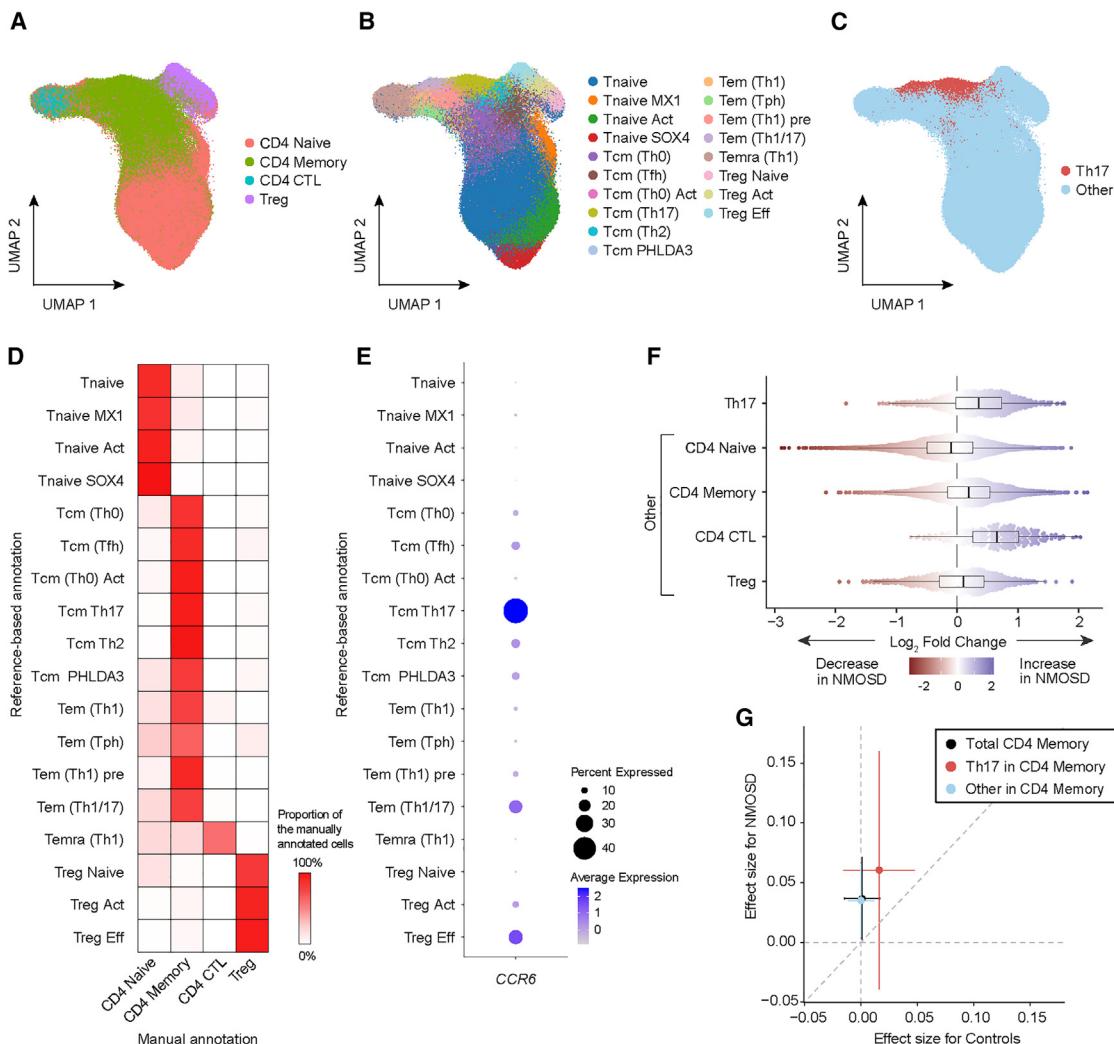
Figure 4. Identification of Th17 cells among CD4T cells and eQTL analysis using Th17 cells

(A–C) Uniform manifold approximation and projection (UMAP) visualization of 372,313 CD4T cells projected onto the reference dataset: manually annotated (the same as Figure 3A) in (A), annotated based on the reference data in (B), and annotated to indicate whether Th17 or other cell types in (C).

(D) Tile plot showing the proportion of the manually annotated four cell types in the reference-based 18 cell types.

(E) Percentage of *CCR6*-expressing cells and *CCR6* expression levels in the 18 reference-based cell types.

(F) Beeswarm plot showing the distribution of adjusted $\log_2$ fold change in abundance between NMOSD and controls in Nhoods according to Th17 cells and other cell types excluding Th17 cells. Boxes denote the interquartile range, and vertical lines denote the median. Whiskers extend to 1.5 times the interquartile range.

(G) Correlations of the eQTL effect sizes of rs12193698 and 95% confidence intervals between NMOSD and healthy controls in CD4 memory cells. The plot includes all CD4 memory cells (black), Th17 cells in CD4 memory cells (red), and CD4 memory cells excluding Th17 cells (light blue).

infections.[16] In this study, we propose the strong association between mCAs and a rare autoimmune disease, NMOSD. Although the previous study[17] showed an association between RA and gene-level mutations, other autoimmune diseases besides NMOSD were not associated with mCAs in our study. This suggests that mCAs may play a unique role in NMOSD, a non-malignant yet deleterious disease. We dissected the somatically mutated cells with loss of 21q, one of the NMO-specific regions,

Figure 3. Cell-type- and disease-specific expression profiles of *CCR6*

Regional association plots of HLA variants with NMOSD risk NMOSD GWAS meta-analysis of Japanese individuals.

(A) Uniform manifold approximation and projection (UMAP) visualization of 1,004,361 PBMCs from the NMOSD cases (*n* = 25) and healthy controls (*n* = 101).

(B) Cell-type-specific expression of *CCR6*.

(C) Percentage of *CCR6*-expressing cells and *CCR6* expression levels in each cell type.

(D) The disease-specific eQTL effects of the *CCR6* risk variant in five cell types. Boxes denote the interquartile range, and horizontal lines denote the median. Whiskers extend to 1.5 times the interquartile range. †FDR <0.1.

(E) Correlations of the eQTL effect sizes of rs12193698 and 95% confidence intervals between NMOSD and healthy controls.

A

B

C

mNMOSD1 (21q loss)

D

E

F

G

Downregulated pathways in CD4T with 21q loss
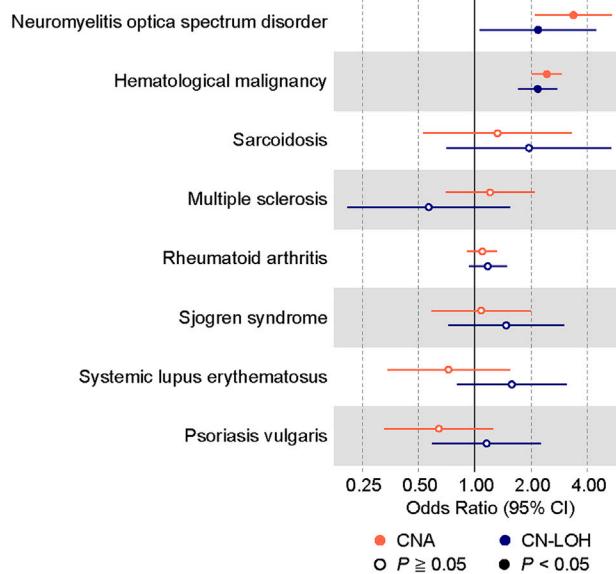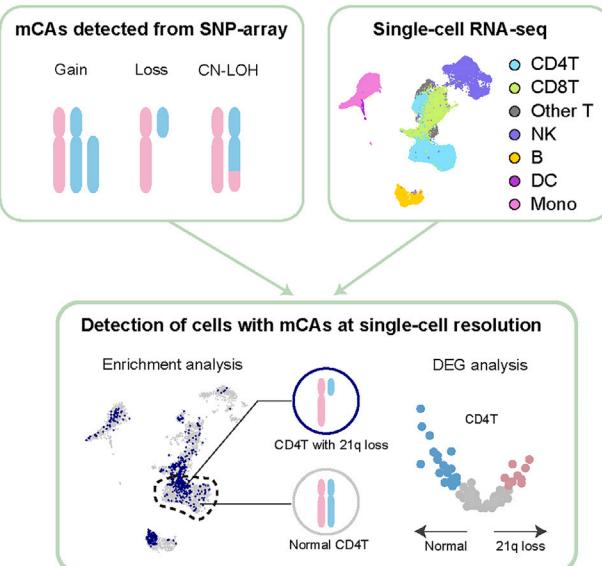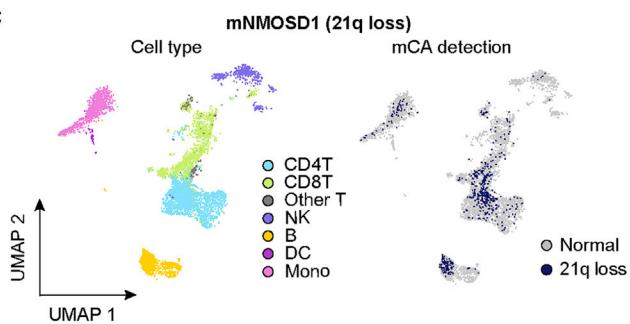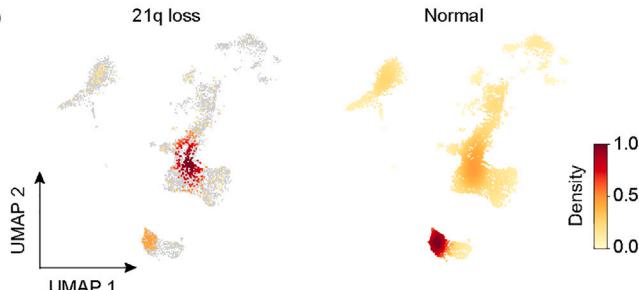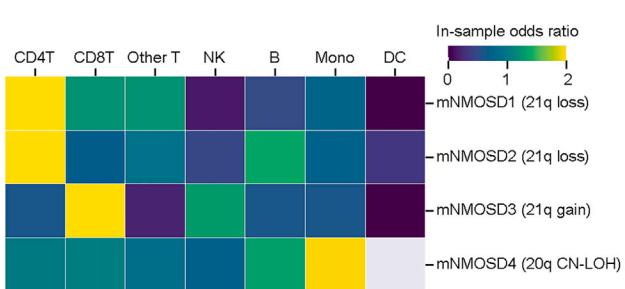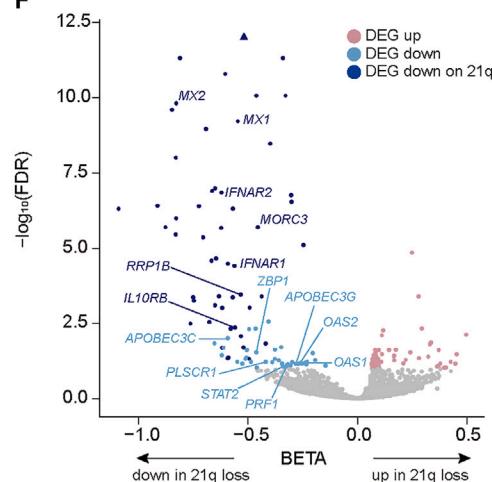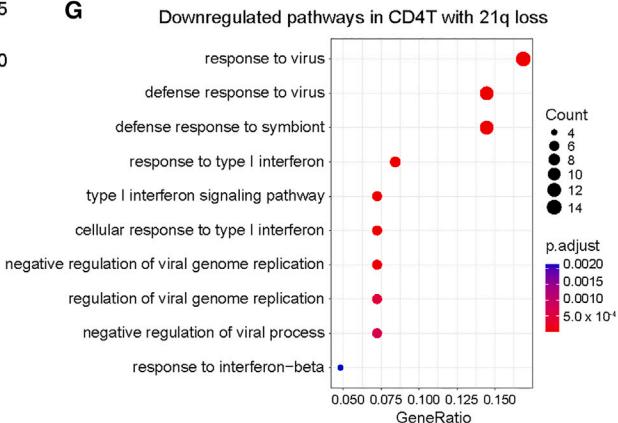
(legend on next page)

at single-cell resolution. Our results showed that this somatic mutation might drive immune system dysregulation through IFN-I signaling. IFN-I has both pro- and anti-inflammatory functions, depending on the pathologic context[47,48]: interferon beta, a member of IFN-I, stimulates B cells to produce inflammatory cytokines,[49] while reduces differentiation of inflammatory T cells.[23] Combining genotype and scRNA-seq data, we revealed the functional impacts of somatic mutations on immune cells and the potential mechanisms underlying their strong association with NMOSD. Our integrated study expands our understanding of the NMOSD genetics from germline variations to somatic mutations.

Limitations of the study
This study has some limitations that should be considered. Our scRNA-seq dataset was generated from PBMCs and did not include macrophages or granulocytes. To further expand our understanding of immune-related cells in NMOSD, future research incorporating these cells would be warranted.

Furthermore, most NMOSD cases included in single-cell analysis were in the remission phase. Investigating samples, including cerebrospinal fluid, from patients in the initial onset or the relapse phase could provide more detailed insights into the mechanisms underlying CNS damage.

RESOURCE AVAILABILITY

Lead contact
Further information and requests for resources and reagents should be directed to and will be fulfilled by the lead contact, Yukinori Okada (yuki-okada@m.u-tokyo.ac.jp).

Materials availability
This study did not generate new unique reagents.

Data and code availability
Summary statistics of the genome-wide meta-analysis have been deposited in the National Bioscience Database Center (NBDC) Human Database (https://humandbs.dbcls.jp/en/) under accession code hum0197 (https://humandbs.dbcls.jp/en/hum0197-latest). Integrated scRNA-seq data including 25 NMOSD cases have been deposited in the Genomic Expression Archive (GEA) (https://www.ddbj.nig.ac.jp/gea/) under accession number E-GEAD-887 (https://ddbj.nig.ac.jp/public/ddbj_database/gea/experiment/E-GEAD-000/E-GEAD-887/). This paper does not report the original code. Any additional information required to reanalyze the data reported in this work is available from the lead contact upon request.

CONSORTIA

Japan MS/NMOSD biobank: Masaaki Niino, Hikoaki Fukaura, Masami Tanaka, Hirofumi Ochi, Takashi Kanda, Fumitaka Shimizu, Yukio Takeshita, Takanori Yokota, Yoichiro Nishida, Makoto Matsui, Shigemi Nagayama, Katsuichi Miyamoto, Masanori Mizuno, Masako Suzuki, Izumi Kawachi, Etsuji Saji, Takashi Ohashi, Shin Hisahara, Kazutoshi Nishiyama, Takahiro Iizuka, Yuji Nakatsuji, Tatsusada Okuno, Takamichi Sugimoto, Kazuhide Ochi, Ryuichi Sakate, Makoto Hirata, Yuko Shimizu, Ryotaro Ikeguchi, Akiko Nagaishi, Kazumasa Okada, Mitsuru Watanabe, Takuya Matsushita, Noriko Isobe, and Jun-ichi Kira

The Biobank Japan Project: Koichi Matsuda, Yuji Yamanashi, Yoichi Furukawa, Takayuki Morisaki, Yukinori Okada, Yoshinori Murakami, Yoichiro Kamatani, Kaori Muto, Akiko Nagai, Yusuke Nakamura, Wataru Obara, Ken Yamaji, Kazuhisa Takahashi, Satoshi Asai, Yasuo Takahashi, Shinichi Higashiue, Shuzo Kobayashi, Hiroki Yamaguchi, Yasunobu Nagata, Satoshi Wakita, Chikako Nito, Yu-ki Iwasaki, Shigeo Murayama, Kozo Yoshimori, Yoshio Miki, Daisuke Obata, Masahiko Higashiyama, Akihide Masumoto, Yoshinobu Koga, and Yukihiro Koretsune

Japan COVID-19 Task Force: Qingbo S. Wang, Ryuya Edahiro, Ho Namkoong, Takanori Hasegawa, Yuya Shirai, Kyuto Sonehara, Hiromu Tanaka, Ho Lee, Ryunosuke Saiki, Takayoshi Hyugaji, Eigo Shimizu, Kotoe Katayama, Masahiro Kanai, Tatsuhiko Naito, Noah Sasa, Kenichi Yamamoto, Yasuhiro Kato, Takayoshi Morita, Kazuhisa Takahashi, Norihiro Harada, Toshio Naito, Makoto Hiki, Yasushi Matsushita, Haruhi Takagi, Masako Ichikawa, Ai Nakamura, Sonoko Harada, Yuuki Sandhu, Hiroki Kabata, Katsunori Masaki, Hirofumi Kamata, Shinnosuke Ikemura, Shotaro Chubachi, Satoshi Okamori, Hideki Terai, Atsuho Morita, Takanori Asakura, Junichi Sasaki, Hiroshi Morisaki, Yoshifumi Uwamino, Kosaku Nanki, Sho Uchid, Shunsuke Uno, Tomoyasu Nishimura, Takashi Ishiguro, Taisuke Isono, Shun Shibata, Yuma Matsui, Chiaki Hosoda, Kenji Takano, Takashi Nishida, Yoichi Kobayashi, Yotaro Takaku, Noboru Takayanagi, Soichiro Ueda, Ai Tada, Masayoshi Miyawaki, Masaomi Yamamoto, Eriko Yoshida, Reina Hayashi, Tomoki Nagasaka, Sawako Arai, Yutaro Kaneko, Kana Sasaki, Etsuko Tagaya, Masatoshi Kawana, Ken Arimura, Kunihiko Takahashi, Tatsuhiko Anzai, Satoshi Ito, Akifumi Endo, Yuji Uchimura, Yasunari Miyazaki, Takayuki Honda, Tomoya Tateishi, Shuji Tohda, Naoya Ichimura, Kazunari Sonobe, Chihiro Tani Sassa, Jun Nakajima, Yasushi Nakano, Yukiko Nakajima, Ryusuke Anan, Ryosuke Arai,

---

Figure 5. Integrated analysis into the association between somatic mutations and NMOSD
(A) Forest plot of the associations between disease risks and mCAs (CNA and CN-LOH). The odds ratios and 95% confidence intervals were calculated using a multivariate logistic regression adjusted for age and sex.
(B) Schematic overview of our integrated analysis of genomics and single-cell transcriptomics.
(C) Uniform manifold approximation and projection (UMAP) embeddings of mNMOSD1 scRNA-seq data colored by cell type (left) and clone (right).
(D) UMAP embeddings of mNMOSD1 scRNA-seq data colored by the density of the 21q loss cells (left) and normal cells (right).
(E) Heatmap showing in-sample odds ratios of each cell type containing mutated cells. Dendritic cells (DCs) in mNMOSD4 are masked in gray due to a limited cell count (<5).
(F) DEG analysis between the 21q loss and normal CD4T cells in mNMOSD1 and mNMOSD2. Significant DEGs satisfying FDR (adjusted p values via the Benjamini-Hochberg method) < 0.1 are colored in light blue or pink, and DEGs on 21q are colored in navy. The upward triangle denotes a data point beyond the axis limit. The genes included in the "response to virus" pathway were annotated.
(G) Top 10 enriched biological pathways of the downregulated DEGs in CD4T cells with 21q loss. The dot color indicates the adjusted enrichment p values via the Benjamini-Hochberg method, and the dot size represents the gene count annotated to each term.

Yuko Kurihara, Yuko Harada, Kazumi Nishio, Tetsuya Ueda, Masanori Azuma, Ryuichi Saito, Toshikatsu Sado, Yoshimune Miyazaki, Ryuichi Sato, Yuki Haruta, Tadao Nagasaki, Yoshinori Yasui, Yoshinori Hasegawa, Yoshikazu Mutoh, Tomoki Kimura, Tomonori Sato, Reoto Takei, Satoshi Hagimoto, Yoichiro Noguchi, Yasuhiko Yamano, Hajime Sasano, Sho Ota, Yasushi Nakamori, Kazuhisa Yoshiya, Fukuki Saito, Tomoyuki Yoshihara, Daiki Wada, Hiromu Iwamura, Syuji Kanayama, Shuhei Maruyama, Takashi Yoshiyama, Ken Ohta, Hiroyuki Kokuto, Hideo Ogata, Yoshiaki Tanaka, Kenichi Arakawa, Masafumi Shimoda, Takeshi Osawa, Hiroki Tateno, Isano Hase, Shuichi Yoshida, Shoji Suzuki, Miki Kawada, Hirohisa Horinouchi, Fumitake Saito, Keiko Mitamura, Masao Hagihara, Junichi Ochi, Tomoyuki Uchida, Rie Baba, Daisuke Arai, Takayuki Ogura, Hidenori Takahashi, Shigehiro Hagiwara, Genta Nagao, Shunichiro Konishi, Ichiro Nakachi, Koji Murakami, Mitsuhiro Yamada, Hisatoshi Sugiura, Hirohito Sano, Shuichiro Matsumoto, Nozomu Kimura, Yoshinao Ono, Hiroaki Baba, Yusuke Suzuki, Sohei Nakayama, Keita Masuzawa, Shinichi Namba, Takayuki Shiroyama, Yoshimi Noda, Takayuki Niitsu, Yuichi Adachi, Takatoshi Enomoto, Saori Amiya, Reina Hara, Yuta Yamaguchi, Teruaki Murakami, Tomoki Kuge, Kinnosuke Matsumoto, Yuji Yamamoto, Makoto Yamamoto, Midori Yoneda, Kazunori Tomono, Kazuto Kato, Haruhiko Hirata, Yoshito Takeda, Hidefumi Koh, Tadashi Manabe, Yohei Funatsu, Fumimaro Ito, Takahiro Fukui, Keisuke Shinozuka, Sumiko Kohashi, Masatoshi Miyazaki, Tomohisa Shoko, Mitsuaki Kojima, Tomohiro Adachi, Motonao Ishikawa, Kenichiro Takahashi, Takashi Inoue, Toshiyuki Hirano, Keigo Kobayashi, Hatsuyo Takaoka, Kazuyoshi Watanabe, Naoki Miyazawa, Yasuhiro Kimura, Reiko Sado, Hideyasu Sugimoto, Akane Kamiya, Naota Kuwahara, Akiko Fujiwara, Tomohiro Matsunaga, Yoko Sato, Takenori Okada, Yoshihiro Hirai, Hidetoshi Kawashima, Atsuya Narita, Kazuki Niwa, Yoshiyuki Sekikawa, Koichi Nishi, Masaru Nishitsuji, Mayuko Tani, Junya Suzuki, Hiroki Nakatsumi, Takashi Ogura, Hideya Kitamura, Eri Hagiwara, Kota Murohashi, Hiroko Okabayashi, Takao Mochimaru, Shigenari Nukaga, Ryosuke Satomi, Yoshitaka Oyamada, Nobuaki Mori, Tomoya Baba, Yasutaka Fukui, Mitsuru Odate, Shuko Mashimo, Yasushi Makino, Kazuma Yagi, Mizuha Hashiguchi, Junko Kagyo, Tetsuya Shiomi, Satoshi Fuke, Hiroshi Saito, Tomoya Tsuchida, Shigeki Fujitani, Mumon Takita, Daiki Morikawa, Toru Yoshida, Takehiro Izumo, Minoru Inomata, Naoyuki Kuse, Nobuyasu Awano, Mari Tone, Akihiro Ito, Yoshihiko Nakamura, Kota Hoshino, Junichi Maruyama, Hiroyasu Ishikura, Tohru Takata, Toshio Odani, Masaru Amishima, Takeshi Hattori, Yasuo Shichinohe, Takashi Kagaya, Toshiyuki Kita, Kazuhide Ohta, Satoru Sakagami, Kiyoshi Koshida, Kentaro Hayashi, Tetsuo Shimizu, Yutaka Kozu, Hisato Hiranuma, Yasuhiro Gon, Namiki Izumi, Kaoru Nagata, Ken Ueda, Reiko Taki, Satoko Hanada, Kodai Kawamura, Kazuya Ichikado, Kenta Nishiyama, Hiroyuki Muranaka, Kazunori Nakamura, Naozumi Hashimoto, Keiko Wakahara, Sakamoto Koji, Norihito Omote, Akira Ando, Nobuhiro Kodama, Yasunari Kaneyama, Shunsuke Maeda, Takashige Kurak, Takemasa Matsumoto, Koutaro Yokote, Taka-Aki Nakada, Ryuzo Abe, Taku Oshima, Tadanaga Shimada, Masahiro Harada, Takeshi Takahashi, Hiroshi Ono, Toshihiro Sakurai, Takayuki Shibusawa, Yoshifumi Kimizuka, Akihiko Kawana, Tomoya Sano, Chie Watanabe, Ryohei Suematsu, Hisako Sageshima, Ayumi Yoshifuji, Kazuto Ito,

Saeko Takahashi, Kota Ishioka, Morio Nakamura, Makoto Masuda, Aya Wakabayashi, Hiroki Watanabe, Suguru Ueda, Masanori Nishikawa, Yusuke Chihara, Mayumi Takeuchi, Keisuke Onoi, Jun Shinozuka, Atsushi Sueyoshi, Yoji Nagasaki, Masaki Okamoto, Sayoko Ishihara, Masatoshi Shimo, Yoshihisa Tokunaga, Yu Kusaka, Takehiko Ohba, Susumu Isogai, Aki Ogawa, Takuya Inoue, Satoru Fukuyama, Yoshihiro Eriguchi, Akiko Yonekawa, Keiko Kan-o, Koichiro Matsumoto, Kensuke Kanaoka, Shoichi Ihara, Kiyoshi Komuta, Yoshiaki Inoue, Shigeru Chiba, Kunihiro Yamagata, Yuji Hiramatsu, Hirayasu Kai, Koichiro Asano, Tsuyoshi Oguma, Yoko Ito, Satoru Hashimoto, Masaki Yamasaki, Yu Kasamatsu, Yuko Komase, Naoya Hida, Takahiro Tsuburai, Baku Oyama, Minoru Takada, Hidenori Kanda, Yuichiro Kitagawa, Tetsuya Fukuta, Takahito Miyake, Shozo Yoshida, Shinji Ogura, Shinji Abe, Yuta Kono, Yuki Togashi, Hiroyuki Takoi, Ryota Kikuchi, Shinichi Ogawa, Tomouki Ogata, Shoichiro Ishihara, Arihiko Kanehiro, Shinji Ozaki, Yasuko Fuchimoto, Sae Wada, Nobukazu Fujimoto, Kei Nishiyama, Mariko Terashima, Satoru Beppu, Kosuke Yoshida, Osamu Narumoto, Hideaki Nagai, Nobuharu Ooshima, Mitsuru Motegi, Akira Umeda, Kazuya Miyagawa, Hisato Shimada, Mayu Endo, Yoshiyuki Ohira, Masafumi Watanabe, Sumito Inoue, Akira Igarashi, Masamichi Sato, Hironori Sagara, Akihiko Tanaka, Shin Ohta, Tomoyuki Kimura, Yoko Shibata, Yoshinori Tanino, Takefumi Nikaido, Hiroyuki Minemura, Yuki Sato, Yuichiro Yamada, Takuya Hashino, Masato Shinoki, Hajime Iwagoe, Hiroshi Takahashi, Kazuhiko Fujii, Hiroto Kishi, Masayuki Kanai, Tomonori Imamura, Tatsuya Yamashita, Masakiyo Yatomi, Toshitaka Maeno, Shinichi Hayashi, Mai Takahashi, Mizuki Kuramochi, Isamu Kamimaki, Yoshiteru Tominaga, Tomoo Ishii, Mitsuyoshi Utsugi, Akihiro Ono, Toru Tanaka, Takeru Kashiwada, Kazue Fujita, Yoshinobu Saito, Masahiro Seike, Hiroko Watanabe, Hiroto Matsuse, Norio Kodaka, Chihiro Nakano, Takeshi Oshio, Takatomo Hirouchi, Shohei Makino, Moritoki Egi, Yosuke Omae, Yasuhito Nannya, Takafumi Ueno, Tomomi Takano, Kazuhiko Katayama, Masumi Ai, Atsushi Kumanogoh, Toshiro Sato, Naoki Hasegawa, Katsushi Tokunaga, Makoto Ishii, Ryuji Koike, Yuko Kitagawa, Akinori Kimura, Seiya Imoto, Satoru Miyano, Seishi Ogawa, Takanori Kanai, Koichi Fukunaga, and Yukinori Okada

AUTHOR CONTRIBUTIONS

Conceptualization, T.Y., G.S., K.O., and Y.O.; investigation, T.Y., G.S., T. Naito, K.S., R.S., R.E., S. Namba, T. Nakanishi, and Y.Y.; resources, T.Y., K.O., R.E., M.W., Y. Shirai, K.Y., H.N., A.H., M.Y., Japan MS/NMOSD biobank, TheBioBank Japan Project, Japan COVID-19 Task Force, E.O.-I., T. Nii, Y.M., K.N., R.N., H.T., S. Nakayamada, K. Matsuda, C.N., S.S., M.K., R.K., A. Kimura, S.I., S.M., K.F., M.M., Y. Shimizu, I.K., K. Miyamoto, Y.T., M.N., Y.N., T.M., J.-I.K., N.I., and T.O.; writing – original draft, T.Y., G.S., K.O., T. Naito, and Y.O.; writing – review & editing, T.Y., G.S., K.O., R.E., and Y.O.; supervision, S.O., A. Kumanogoh, J.K., H.M., N.I., T.O., and Y.O.

DECLARATION OF INTERESTS

The authors declare no competing interests.

STAR★METHODS

Detailed methods are provided in the online version of this paper and include the following:

- KEY RESOURCES TABLE
- EXPERIMENTAL MODEL AND STUDY PARTICIPANT DETAILS
  - The participants for genome-wide association study
- SUBJECTS AND SPECIMEN COLLECTION OF PBMC FOR SCRNA-SEQ
- METHOD DETAILS
  - Genotyping and quality control
  - Genotype imputation
  - Genome-wide association study
  - Comparison with other autoimmune diseases study
  - HLA imputation and association study
  - Droplet-based single-cell sequencing
  - Alignment, quantification, and quality control of scRNA-seq data
  - scRNA-seq computation pipelines
  - Differential expression analysis using scRNA-seq data
  - Single-cell eQTL analysis
  - Cell-cell interaction analysis in PBMCs
  - Reference-based annotation of CD4T cells
  - Differential abundance analysis
  - pQTL analysis
  - Associations between disease risks and mCAs
  - Single-cell dissection of somatically mutated cells in NMOSD patients
- QUANTIFICATION AND STATISTICAL ANALYSIS

SUPPLEMENTAL INFORMATION

Supplemental information can be found online at https://doi.org/10.1016/j.xgen.2025.100776.

REFERENCES

1. Wingerchuk, D.M., Banwell, B., Bennett, J.L., Cabre, P., Carroll, W., Chitnis, T., De Seze, J., Fujihara, K., Greenberg, B., Jacob, A., et al. (2015). International consensus diagnostic criteria for neuromyelitis optica spectrum disorders. Neurology 85, 177–189.

2. Huda, S., Whittam, D., Bhojak, M., Chamberlain, J., Noonan, C., and Jacob, A. (2019). Neuromyelitis optica spectrum disorders. Clin. Med. 19, 169–176.

3. Lennon, V.A., Wingerchuk, D.M., Kryzer, T.J., Pittock, S.J., Lucchinetti, C.F., Fujihara, K., Nakashima, I., and Weinshenker, B.G. (2004). A serum autoantibody marker of neuromyelitis optica: distinction from multiple sclerosis. Lancet 364, 2106–2112.

4. Papadopoulos, M.C., and Verkman, A.S. (2012). Aquaporin 4 and neuromyelitis optica. Lancet Neurol. 11, 535–544.

5. Hor, J.Y., Asgari, N., Nakashima, I., Broadley, S.A., Leite, M.I., Kissani, N., Jacob, A., Marignier, R., Weinshenker, B.G., Paul, F., et al. (2020). Epidemiology of Neuromyelitis Optica Spectrum Disorder and Its Prevalence and Incidence Worldwide. Front. Neurol. 11, 501.

6. Kim, H.J., Park, H.Y., Kim, E., Lee, K.S., Kim, K.K., Choi, B.O., Kim, S.M., Bae, J.S., Lee, S.O., Chun, J.Y., et al. (2010). Common CYP7A1 promoter polymorphism associated with risk of neuromyelitis optica. Neurobiol. Dis. 37, 349–355.

7. Estrada, K., Whelan, C.W., Zhao, F., Bronson, P., Handsaker, R.E., Sun, C., Carulli, J.P., Harris, T., Ransohoff, R.M., McCarroll, S.A., et al. (2018). A whole-genome sequence study identifies genetic risk factors for neuromyelitis optica. Nat. Commun. 9, 1929.

8. Matsushita, T., Masaki, K., Isobe, N., Sato, S., Yamamoto, K., Nakamura, Y., Watanabe, M., Suenaga, T., and Kira, J.I.; Japan Multiple Sclerosis Genetic Consortium (2020). Genetic factors for susceptibility and manifestations of neuromyelitis optica. Ann. Clin. Transl. Neurol. 7, 2082–2093.

9. Ogawa, K., Okuno, T., Hosomichi, K., Hosokawa, A., Hirata, J., Suzuki, K., Sakaue, S., Kinoshita, M., Asano, Y., Miyamoto, K., et al. (2019). Next-generation sequencing identifies contribution of both class I and II HLA genes on susceptibility of multiple sclerosis in Japanese. J. Neuroinflammation 16, 162.

10. Watanabe, M., Nakamura, Y., Sato, S., Niino, M., Fukaura, H., Tanaka, M., Ochi, H., Kanda, T., Takeshita, Y., Yokota, T., et al. (2021). HLA genotype-clinical phenotype correlations in multiple sclerosis and neuromyelitis optica spectrum disorders based on Japan MS/NMOSD Biobank data. Sci. Rep. 11, 607.

11. Loh, P.R., Genovese, G., Handsaker, R.E., Finucane, H.K., Reshef, Y.A., Palamara, P.F., Birmann, B.M., Talkowski, M.E., Bakhoum, S.F., McCarroll, S.A., and Price, A.L. (2018). Insights into clonal haematopoiesis from 8,342 mosaic chromosomal alterations. Nature 559, 350–355.

12. Loh, P.R., Genovese, G., and McCarroll, S.A. (2020). Monogenic and polygenic inheritance become instruments for clonal selection. Nature 584, 136–141.

13. Laurie, C.C., Laurie, C.A., Rice, K., Doheny, K.F., Zelnick, L.R., McHugh, C.P., Ling, H., Hetrick, K.N., Pugh, E.W., Amos, C., et al. (2012). Detectable clonal mosaicism from birth to old age and its relationship to cancer. Nat. Genet. 44, 642–650.

14. Niroula, A., Sekar, A., Murakami, M.A., Trinder, M., Agrawal, M., Wong, W.J., Bick, A.G., Uddin, M.M., Gibson, C.J., Griffin, G.K., et al. (2021). Distinction of lymphoid and myeloid clonal hematopoiesis. Nat. Med. 27, 1921–1927.

15. Saiki, R., Momozawa, Y., Nannya, Y., Nakagawa, M.M., Ochi, Y., Yoshizato, T., Terao, C., Kuroda, Y., Shiraishi, Y., Chiba, K., et al. (2021). Combined landscape of single-nucleotide variants and copy number alterations in clonal hematopoiesis. Nat. Med. 27, 1239–1249.

16. Zekavat, S.M., Lin, S.H., Bick, A.G., Liu, A., Paruchuri, K., Wang, C., Uddin, M.M., Ye, Y., Yu, Z., Liu, X., et al. (2021). Hematopoietic mosaic chromosomal alterations increase the risk for diverse types of infection. Nat. Med. 27, 1012–1024.

17. Hiitola, E., Korhonen, J., Koskela, J., Kankainen, M., Alakuijala, M., Kokkonen, H., Liu, A., Häppölä, P., Savola, P., Kelkka, T., et al. (2023). Clonal Hematopoiesis Associated with Rheumatoid Arthritis. Blood 142, 2698.

18. Nam, A.S., Dusaj, N., Izzo, F., Murali, R., Myers, R.M., Mouhieddine, T.H., Sotelo, J., Benbarche, S., Waarts, M., Gaiti, F., et al. (2022). Single-cell multi-omics of human clonal hematopoiesis reveals that DNMT3A R882 mutations perturb early progenitor states through selective hypomethylation. Nat. Genet. 54, 1514–1526.

19. Gao, T., Kastriti, M.E., Ljungström, V., Heinzel, A., Tischler, A.S., Oberbauer, R., Loh, P.R., Adameyko, I., Park, P.J., and Kharchenko, P.V. (2023). A pan-tissue survey of mosaic chromosomal alterations in 948 individuals. Nat. Genet. *55*, 1901–1911.

20. Nagai, A., Hirata, M., Kamatani, Y., Muto, K., Matsuda, K., Kiyohara, Y., Ninomiya, T., Tamakoshi, A., Yamagata, Z., Mushiroda, T., et al. (2017). Overview of the BioBank Japan Project: Study design and profile. J. Epidemiol. *27*, S2–S8.

21. Schutyser, E., Struyf, S., and Van Damme, J. (2003). The CC chemokine CCL20 and its receptor CCR6. Cytokine Growth Factor Rev. *14*, 409–426.

22. Yamazaki, T., Yang, X.O., Chung, Y., Fukunaga, A., Nurieva, R., Pappu, B., Martin-Orozco, N., Kang, H.S., Ma, L., Panopoulos, A.D., et al. (2008). CCR6 Regulates the Migration of Inflammatory and Regulatory T Cells. J. Immunol. *181*, 8391–8401.

23. Axtell, R.C., De Jong, B.A., Boniface, K., Van Der Voort, L.F., Bhat, R., De Sarno, P., Naves, R., Han, M., Zhong, F., Castellanos, J.G., et al. (2010). T helper type 1 and 17 cells determine efficacy of interferon-B in multiple sclerosis and experimental encephalomyelitis. Nat. Med. *16*, 406–412.

24. Uzawa, A., Mori, M., Ito, M., Uchida, T., Hayakawa, S., Masuda, S., and Kuwabara, S. (2009). Markedly increased CSF interleukin-6 levels in neuromyelitis optica, but not in multiple sclerosis. J. Neurol. *256*, 2082–2084.

25. Varrin-Doyer, M., Spencer, C.M., Schulze-Topphoff, U., Nelson, P.A., Stroud, R.M., Cree, B.A.C., and Zamvil, S.S. (2012). Aquaporin 4-specific T cells in neuromyelitis optica exhibit a Th17 bias and recognize Clostridium ABC transporter. Ann. Neurol. *72*, 53–64.

26. Kochi, Y., Okada, Y., Suzuki, A., Ikari, K., Terao, C., Takahashi, A., Yamazaki, K., Hosono, N., Myouzen, K., Tsunoda, T., et al. (2010). A regulatory variant in CCR6 is associated with rheumatoid arthritis susceptibility. Nat. Genet. *42*, 515–519.

27. Ishigaki, K., Sakaue, S., Terao, C., Luo, Y., Sonehara, K., Yamaguchi, K., Amariuta, T., Too, C.L., Laufer, V.A., Scott, I.C., et al. (2022). Multi-ancestry genome-wide association analyses identify novel genetic mechanisms in rheumatoid arthritis. Nat. Genet. *54*, 1640–1651.

28. Cordell, H.J., Fryett, J.J., Ueno, K., Darlay, R., Aiba, Y., Hitomi, Y., Kawashima, M., Nishida, N., Khor, S.S., Gervais, O., et al. (2021). An international genome-wide meta-analysis of primary biliary cholangitis: Novel risk loci and candidate drugs. J. Hepatol. *75*, 572–581.

29. Pereira, W.L.D.C.J., Reiche, E.M.V., Kallaur, A.P., Oliveira, S.R., Simão, A.N.C., Lozovoy, M.A.B., Schiavão, L.J.V., Rodrigues, P.R.D.V.P., Alfieri, D.F., Flauzino, T., and Kaimen-Maciel, D.R. (2017). Frequency of autoimmune disorders and autoantibodies in patients with neuromyelitis optica. Acta Neuropsychiatr. *29*, 170–178.

30. Zhao, M., Zhang, M., Zhou, S., Shi, B., Wei, Y., Huang, F., Wang, J., Huang, J., and Qiao, L. (2022). Transverse myelitis associated with primary biliary cirrhosis: clinical, laboratory, and neuroradiological features. Int. J. Neurosci. *132*, 370–377.

31. Adawi, M., Bisharat, B., and Bowirrat, A. (2014). Systemic lupus erythematosus (SLE) complicated by neuromyelitis optica (NMO - devic's disease): Clinic-pathological report and review of the literature. Clin. Med. Insights Case Rep. *7*, 41–47.

32. Yin, X., Kim, K., Suetsugu, H., Bang, S.Y., Wen, L., Koido, M., Ha, E., Liu, L., Sakamoto, Y., Jo, S., et al. (2021). Meta-analysis of 208370 East Asians identifies 113 susceptibility loci for systemic lupus erythematosus. Ann. Rheum. Dis. *80*, 632–640.

33. Hao, Y., Hao, S., Andersen-Nissen, E., Mauck, W.M., Zheng, S., Butler, A., Lee, M.J., Wilk, A.J., Darby, C., Zager, M., et al. (2021). Integrated analysis of multimodal single-cell data. Cell *184*, 3573–3587.e29.

34. Lee, A.Y.S., Eri, R., Lyons, A.B., Grimm, M.C., and Korner, H. (2013). CC chemokine ligand 20 and its cognate receptor CCR6 in mucosal T cell immunology and inflammatory bowel disease: Odd couple or axis of evil? Front. Immunol. *4*, 194.

35. Jin, S., Guerrero-Juarez, C.F., Zhang, L., Chang, I., Ramos, R., Kuan, C.H., Myung, P., Plikus, M.V., and Nie, Q. (2021). Inference and analysis of cell-cell communication using CellChat. Nat. Commun. *12*, 1088.

36. Yasumizu, Y., Takeuchi, D., Morimoto, R., Takeshima, Y., Okuno, T., Kinoshita, M., Morita, T., Kato, Y., Wang, M., Motooka, D., et al. (2024). Single-cell transcriptome landscape of circulating CD4+ T cell populations in autoimmune diseases. Cell Genom. *4*, 100473.

37. Wang, Q.S., Edahiro, R., Namkoong, H., Hasegawa, T., Shirai, Y., Sonehara, K., Tanaka, H., Lee, H., Saiki, R., Hyugaji, T., et al. (2022). The whole blood transcriptional regulation landscape in 465 COVID-19 infected samples from Japan COVID-19 Task Force. Nat. Commun. *13*, 4830.

38. Namkoong, H., Edahiro, R., Takano, T., Nishihara, H., Shirai, Y., Sonehara, K., Tanaka, H., Azekawa, S., Mikami, Y., Lee, H., et al. (2022). DOCK2 is involved in the host genetics and biology of severe COVID-19. Nature *609*, 754–760.

39. Wang, Q.S., Hasegawa, T., Namkoong, H., Saiki, R., Edahiro, R., Sonehara, K., Tanaka, H., Azekawa, S., Chubachi, S., Takahashi, Y., et al. (2024). Statistically and functionally fine-mapped blood eQTLs and pQTLs from 1,405 humans reveal distinct regulation patterns and disease relevance. Nat. Genet. *56*, 2054–2067.

40. Greulich, W., Wagner, M., Gaidt, M.M., Stafford, C., Cheng, Y., Linder, A., Carell, T., and Hornung, V. (2019). TLR8 Is a Sensor of RNase T2 Degradation Products. Cell *179*, 1264–1275.e13.

41. Cervantes, J.L., Weinerman, B., Basole, C., and Salazar, J.C. (2012). TLR8: The forgotten relative revindicated. Cell. Mol. Immunol. *9*, 434–438.

42. Johnson, T.P., Tyagi, R., Patel, K., Schiess, N., Calabresi, P.A., and Nath, A. (2013). Impaired toll-like receptor 8 signaling in multiple sclerosis. J. Neuroinflammation *10*, 74.

43. Gao, T., Soldatov, R., Sarkar, H., Kurkiewicz, A., Biederstedt, E., Loh, P.R., and Kharchenko, P.V. (2023). Haplotype-aware analysis of somatic copy number variations from single-cell transcriptomes. Nat. Biotechnol. *41*, 417–426.

44. Kebir, H., Kreymborg, K., Ifergan, I., Dodelet-Devillers, A., Cayrol, R., Bernard, M., Giuliani, F., Arbour, N., Becher, B., and Prat, A. (2007). Human TH17 lymphocytes promote blood-brain barrier disruption and central nervous system inflammation. Nat. Med. *13*, 1173–1175.

45. Arima, Y., Harada, M., Kamimura, D., Park, J.H., Kawano, F., Yull, F.E., Kawamoto, T., Iwakura, Y., Betz, U.A.K., Márquez, G., et al. (2012). Regional neural activation defines a gateway for autoreactive T cells to cross the blood-brain barrier. Cell *148*, 447–457.

46. Ifergan, I., Kébir, H., Bernard, M., Wosik, K., Dodelet-Devillers, A., Cayrol, R., Arbour, N., and Prat, A. (2008). The blood-brain barrier induces differentiation of migrating monocytes into Th17-polarizing dendritic cells. Brain *131*, 785–799.

47. Axtell, R.C., Raman, C., and Steinman, L. (2011). Interferon-β exacerbates Th17-mediated inflammatory disease. Trends Immunol. *32*, 272–277.

48. Kasper, L.H., and Reder, A.T. (2014). Immunomodulatory activity of interferon-beta. Ann. Clin. Transl. Neurol. *1*, 622–631.

49. Agasing, A.M., Wu, Q., Khatri, B., Borisow, N., Ruprecht, K., Brandt, A.U., Gawde, S., Kumar, G., Quinn, J.L., Ko, R.M., et al. (2020). Transcriptomics and proteomics reveal a cooperation between interferon and T-helper 17 cells in neuromyelitis optica. Nat. Commun. *11*, 2856.

50. Tadaka, S., Katsuoka, F., Ueki, M., Kojima, K., Makino, S., Saito, S., Otsuki, A., Gocho, C., Sakurai-Yageta, M., Danjoh, I., et al. (2019). 3.5KJPNv2: an allele frequency panel of 3552 Japanese individuals including the X chromosome. Hum. Genome Var. *6*, 28.

51. Edahiro, R., Shirai, Y., Takeshima, Y., Sakakibara, S., Yamaguchi, Y., Murakami, T., Morita, T., Kato, Y., Liu, Y.-C., Motooka, D., et al. (2023). Single-cell analyses and host genetics highlight the role of innate immune cells in COVID-19 severity. Nat. Genet. *55*, 753–767.

52. Fleming, S.J., Chaffin, M.D., Arduini, A., Akkad, A.D., Banks, E., Marioni, J.C., Philippakis, A.A., Ellinor, P.T., and Babadi, M. (2023). Unsupervised

removal of systematic background noise from droplet-based single-cell experiments using CellBender. Nat. Methods *20*, 1323–1335.

53. Yu, G., Wang, L.G., Han, Y., and He, Q.Y. (2012). ClusterProfiler: An R package for comparing biological themes among gene clusters. OMICS *16*, 284–287.

54. Naito, T., Suzuki, K., Hirata, J., Kamatani, Y., Matsuda, K., Toda, T., and Okada, Y. (2021). A deep learning method for HLA imputation and trans-ethnic MHC fine-mapping of type 1 diabetes. Nat. Commun. *12*, 1639.

55. McGinnis, C.S., Murrow, L.M., and Gartner, Z.J. (2019). DoubletFinder: Doublet Detection in Single-Cell RNA Sequencing Data Using Artificial Nearest Neighbors. Cell Syst. *8*, 329–337.e4.

56. Robinson, M.D., McCarthy, D.J., and Smyth, G.K. (2010). edgeR: A Bio-conductor package for differential expression analysis of digital gene expression data. Bioinformatics *26*, 139–140.

57. Bates, D., Mächler, M., Bolker, B.M., and Walker, S.C. (2015). Fitting linear mixed-effects models using lme4. J Stat Softw *67*, 1–48.

58. Han, B., and Eskin, E. (2011). Random-effects model aimed at discovering associations in meta-analysis of genome-wide association studies. Am. J. Hum. Genet. *88*, 586–598.

59. Dann, E., Henderson, N.C., Teichmann, S.A., Morgan, M.D., and Marioni, J.C. (2022). Differential abundance testing on single-cell data using k-nearest neighbor graphs. Nat. Biotechnol. *40*, 245–253.

60. Purcell, S., Neale, B., Todd-Brown, K., Thomas, L., Ferreira, M.A.R., Bender, D., Maller, J., Sklar, P., De Bakker, P.I.W., Daly, M.J., and Sham, P.C. (2007). PLINK: A tool set for whole-genome association and population-based linkage analyses. Am. J. Hum. Genet. *81*, 559–575.

61. Chang, C.C., Chow, C.C., Tellier, L.C., Vattikuti, S., Purcell, S.M., and Lee, J.J. (2015). Second-generation PLINK: Rising to the challenge of larger and richer datasets. GigaScience *4*, 7.

62. Zhou, W., Nielsen, J.B., Fritsche, L.G., Dey, R., Gabrielsen, M.E., Wolford, B.N., LeFaive, J., VandeHaar, P., Gagliano, S.A., Gifford, A., et al. (2018). Efficiently controlling for case-control imbalance and sample relatedness in large-scale genetic association studies. Nat. Genet. *50*, 1335–1341.

63. Hie, B., Bryson, B., and Berger, B. (2019). Efficient integration of heterogeneous single-cell transcriptomes using Scanorama. Nat. Biotechnol. *37*, 685–691.

64. Wolf, F.A., Angerer, P., and Theis, F.J. (2018). SCANPY: large-scale single-cell gene expression data analysis. Genome Biol. *19*, 15.

65. Sturm, G., Szabo, T., Fotakis, G., Haider, M., Rieder, D., Trajanoski, Z., and Finotello, F. (2020). Scirpy: A Scanpy extension for analyzing single-cell T-cell receptor-sequencing data. Bioinformatics *36*, 4817–4818.

66. Lun, A.T.L., Bach, K., and Marioni, J.C. (2016). Pooling across cells to normalize single-cell RNA sequencing data with many zero counts. Genome Biol. *17*, 75.

67. Delaneau, O., Zagury, J.F., Robinson, M.R., Marchini, J.L., and Dermitza-kis, E.T. (2019). Accurate, scalable and integrative haplotype estimation. Nat. Commun. *10*, 5436.

68. Dobin, A., Davis, C.A., Schlesinger, F., Drenkow, J., Zaleski, C., Jha, S., Batut, P., Chaisson, M., and Gingeras, T.R. (2013). STAR: Ultrafast universal RNA-seq aligner. Bioinformatics *29*, 15–21.

69. Belmont, J.W., Boudreau, A., Leal, S.M., Hardenbol, P., Pasternak, S., Wheeler, D.A., Willis, T.D., Yu, F., Yang, H., Gao, Y., et al. (2005). A haplotype map of the human genome. Nature *437*, 1299–1320.

70. Yamaguchi-Kabata, Y., Nakazono, K., Takahashi, A., Saito, S., Hosono, N., Kubo, M., Nakamura, Y., and Kamatani, N. (2008). Japanese Population Structure, Based on SNP Genotypes from 7003 Individuals Compared to Other Ethnic Groups: Effects on Population-Based Association Studies. Am. J. Hum. Genet. *83*, 445–456.

71. Das, S., Forer, L., Schönherr, S., Sidore, C., Locke, A.E., Kwong, A., Vrieze, S.I., Chew, E.Y., Levy, S., McGue, M., et al. (2016). Next-generation genotype imputation service and methods. Nat. Genet. *48*, 1284–1287.

72. Hirata, J., Hosomichi, K., Sakaue, S., Kanai, M., Nakaoka, H., Ishigaki, K., Suzuki, K., Akiyama, M., Kishikawa, T., Ogawa, K., et al. (2019). Genetic and phenotypic landscape of the major histocompatibilty complex region in the Japanese population. Nat. Genet. *51*, 470–480.

73. Naito, T., and Okada, Y. (2022). HLA imputation and its application to genetic and molecular fine-mapping of the MHC region in autoimmune diseases. Semin. Immunopathol. *44*, 15–28.

STAR★METHODS

KEY RESOURCES TABLE

REAGENT or RESOURCE	SOURCE	IDENTIFIER
Biological samples		
Human DNA extracted from peripheral blood	This study	N/A
Human peripheral blood mononuclear cells	This study	N/A
Deposited data		
Genotype data of BioBank Japan	Nagai et al.[20]	Japanese Genotype-phenotype Archive of Biobank Japan (JGA) with the accession ID JGAS000412, which is available through application at https://humandbs.biosciencedbc.jp/en/hum0311-latest
Allele frequency reference panel of Tohoku Medical Megabank Project	Tadaka et al.[50]	https://jmorp.megabank.tohoku.ac.jp/downloads
Summary statistics of the genome-wide meta-analysis of NMOSD	This study	NBDC: hum0197
Integrated scRNA-seq data including 25 NMOSD cases	This study	GEAD: E-GEAD-887
Japanese scRNA-seq dataset for controls	Edahiro et al.[51]	Japanese Genotype-phenotype Archive (JGA) with the accession ID JGAS000593/JGAD000722/JGAS000543/JGAD000662, which is available through application at https://humandbs.biosciencedbc.jp/en/hum0197-latest
Japanese scRNA-seq dataset of CD4T cells	Yasumizu et al.[36]	https://github.com/yyoshiaki/screfmapping
Software and algorithms		
Azimuth	Hao et al.[33]	https://azimuth.hubmapconsortium.org/
CellBender	Fleming et al.[52]	https://github.com/broadinstitute/CellBender
CellChat	Jin et al.[35]	https://github.com/sqjin/CellChat
Cell Ranger	10x Genomics	https://www.10xgenomics.com/jp/support/software/cell-ranger/latest
Clusterprofiler	Yu et al.[53]	https://github.com/YuLab-SMU/clusterProfiler
DEEP*HLA	Naito et al.[54]	https://github.com/tatsuhikonaito/DEEP-HLA
DoubletFinder	McGinnis et al.[55]	https://github.com/chris-mcginnis-ucsf/DoubletFinder
edgeR	Robinson et al.[56]	https://bioconductor.org/packages/release/bioc/html/edgeR.html
lme4	Bates et al.[57]	https://github.com/lme4/lme4
METASOFT	Han et al.[58]	http://genetics.cs.ucla.edu/meta/
MoChA	Loh et al.[11,12]	https://github.com/freeseek/mocha
Milo	Dann et al.[59]	https://github.com/MarioniLab/miloR
Numbat	Jin et al.[35]	https://kharchenkolab.github.io/numbat/
PLINK	Purcell et al.[60]	https://www.cog-genomics.org/plink/1.9
PLINK2	Chang et al.[61]	https://www.cog-genomics.org/plink/2.0
Python	Python Software Foundation	https://www.python.org/downloads/release/python-376/
R	The R Foundation for Statistical Computing	https://www.r-project.org/
SAIGE	Zhou et al.[62]	https://github.com/weizhouUMICH/SAIGE
Scanorama	Hie et al.[63]	https://github.com/brianhie/scanorama
Scanpy	Wolf et al.[64]	https://scanpy.readthedocs.io/en/stable/
Scirpy	Sturm et al.[65]	https://github.com/scverse/scirpy
scran	Lun et al.[66]	https://bioconductor.org/packages/release/bioc/html/scran.html

(Continued on next page)

Continued

REAGENT or RESOURCE	SOURCE	IDENTIFIER
Seurat	Hao et al.[33]	https://satijalab.org/seurat/
SHAPEIT4	Delaneau et al.[67]	https://github.com/odelaneau/shapeit4
STAR	Dobin et al.[68]	https://github.com/alexdobin/STAR

EXPERIMENTAL MODEL AND STUDY PARTICIPANT DETAILS

The participants for genome-wide association study
Discovery cohort
We obtained DNA samples of 183 neuromyelitis optica spectrum disorder (NMOSD) cases from 18 institutes enrolled in the Japan MS/NMOSD biobank (Kyushu University Hospital, Utano National Hospital, Sapporo Medical University Hospital, Yamaguchi University Hospital, Tokyo Women's Medical University Yachiyo Medical Center, Osaka University Hospital, Tokyo Women's Medical University Hospital, Saitama Medical Center, Hokkaido Medical Center, Ehime University Hospital, Hiroshima University Hospital, Nagasaki Kawatana Medical Center, Tokyo Medical and Dental University Hospital, Kitasato University Hospital, Niigata University Medical and Dental Hospital, Hospital of University of Occupational and Environmental Health, Iwate Medical University Hospital, and Hachinohe Red Cross Hospital) between August 2013 and March 2017. All the subjects agreed with informed consent based on the approval of the institutional ethical committee. We collected 42,689 control subjects from Biobank Japan (BBJ) project.[20] All DNA samples were extracted from peripheral blood.
Replication cohort
We additionally collected 81 samples from patients in Osaka University Hospital and five cooperating institutes (Hokkaido Medical Center, Kindai University Hospital, Tokyo Women's Medical University Hospital, Toyama University Hospital, and Kawasaki Medical School Hospital) between October 2013 and October 2022. All the subjects agreed with informed consent based on the approval of the institutional ethical committee. As controls, we obtained 11,716 samples independent of the discovery cohort from BBJ.[20] All DNA samples were extracted from peripheral blood.

SUBJECTS AND SPECIMEN COLLECTION OF PBMC FOR scRNA-SEQ

Peripheral blood samples were obtained from patients with NMOSD ($n = 25$) and healthy controls ($n = 101$) recruited at Osaka University Hospital. For the detection of chromosomal alterations, we revisited case samples from Osaka University Hospital ($n = 2$), Hokkaido Medical Center ($n = 1$), and Toyama University Hospital ($n = 1$). We collected peripheral blood into heparin tubes and isolated PBMCs using Leucosep (Greiner Bio-One) density gradient centrifugation according to the manufacturer's instructions. We processed blood samples within 3 h of collection and stored them at $-80°$C until use.

METHOD DETAILS

Genotyping and quality control
We performed genotyping of all case and control subjects using Infinium Asian Screening Array (Illumina). We applied the same stringent quality control to both cohorts: we excluded individuals with a low genotyping call rate (<0.98) or potential sex chromosome aneuploidy. We excluded cases which did not meet the 2015 International Panel for NMO Diagnosis criteria.[1] Duplicate samples were excluded based on genotype information (PI_HAT calculated by PLINK version 1.9[60] > 0.75). In both cohorts, we excluded controls with autoimmune or allergic diseases. We included only the individuals of the estimated East Asian ancestry based on the principal component (PC) analysis with the individuals of the HapMap project,[69] and then further restricted to those in Japanese Hondo (the main island of Japan) clusters.[70] Sample filtering resulted in 163 cases and 40,908 controls in the discovery cohort, and 77 cases and 9,670 controls in the replication cohort for association analysis.

As a variant filter, we excluded variants with call rate <0.99, minor allele count <5, p value for Hardy–Weinberg equilibrium $<1.0 \times 10^{-10}$, or >5% allele frequency difference compared to the Tohoku Medical Megabank Project[50] dataset and in-house reference panel described below.

Genotype imputation
We conducted genome-wide genotype imputation to estimate untyped variants. We used the in-house reference panel consisting of Japanese whole-genome sequencing data ($n = 11,754$) as a haplotype reference for genotype imputation. We performed haplotype estimation using SHAPEIT4[67] and then conducted genotype imputation with Minimac4.[71] After the imputation, we extracted the variants imputed with $Rsq > 0.7$ and a minor allele frequency >0.005 for the association analysis.

Genome-wide association study

We conducted a genome-wide association study (GWAS) for each cohort with a generalized linear mixed model implemented in SAIGE (v1.0.0).[62] We included age and the top four PCs as covariates in the regression model, with genetic relation matrix under leave-one-chromosome-out approach. We adopted a genome-wide association significance threshold of $p = 5.0 \times 10^{-8}$. We conducted an inverse variance fixed-effects meta-analysis using METASOFT[58] for GWAS meta-analysis.

Comparison with other autoimmune diseases study

To compare the genetic background of NMOSD and other autoimmune diseases in East Asians, we examined GWAS summary statistics from studies of rheumatoid arthritis (RA),[27] primary biliary cholangitis (PBC),[28] and systemic lupus erythematosus (SLE),[32] in which enough associated variants have been reported. For the RA, PBC, or SLE risk variant ($p < 5.0 \times 10^{-8}$), we assessed their effect sizes in our NMOSD study and examined correlations. We excluded variants in major histocompatibility complex (MHC) (chromosome 6: 25–35 Mbp).

HLA imputation and association study

We performed human leukocyte antigen (HLA) imputation with the HLA reference panel of the Japanese population ($n = 1,118$) constructed in the previous study.[72] We applied Deep*HLA, deep learning-based HLA imputation,[54,73] to the genotyped SNPs in the MHC region and imputed the classical HLA alleles (one- and two-field [two- and four-digit]) and amino acid variants of class I and II HLA genes (*HLA-A*, *HLA-C*, *HLA-B*, *HLA-DRB1*, *HLA-DQA1*, *HLA-DQB1*, *HLA-DPA1*, and *HLA-DPB1*). The variants imputed with an imputation quality score of R^2 in 10-fold cross-validation >0.7 and MAF >0.005 were used for further analyses.

For fine-mapping in MHC, we evaluated associations of the HLA variants with the risk of NMOSD using a logistic regression model using a glm() function implemented in R software (v3.6.0).[54,72] The HLA variants were defined as SNPs in the MHC region, two-digit and four-digit HLA alleles, biallelic HLA amino acid polymorphisms corresponding to their respective residues, and multiallelic HLA amino acid polymorphisms for each amino acid position. For multiallelic amino acid polymorphisms, we estimated their significance using an omnibus test for each amino acid position through a log likelihood ratio test, comparing the likelihood of the fitted model with the null model. The significance of the improvement in model fitting was evaluated by the deviance, which follows a chi-square distribution with $m - 1$ degrees of freedom for an amino acid position with m polymorphic residues. Non-additive effects were tested assessing by the significance of including an interaction term between target variants, as well at these variants, into the model. To evaluate independent risk among and across the HLA genes, we conducted a forward-type stepwise conditional regression analysis that additionally included the associated variant genotypes as covariates. When conditioning a specific HLA gene, we included all the 4-digit alleles of that HLA gene as covariates to robustly condition the associations attributable to it. When conditioning on a specific HLA amino acid position, we included all the amino acid residues belonging to that position with the most frequent one excluded as the reference allele. Given the need to perform the omnibus test, we constructed a model for the combined data from the two cohorts with including a variable representing each cohort as a covariate, instead of conducting a meta-analysis between results from the two cohorts. We used otherwise the same covariates as those used in the GWAS. We adopted a genome-wide association significance threshold of $p = 5.0 \times 10^{-8}$.

Droplet-based single-cell sequencing

We processed single-cell suspension through the 10X Genomics Chromium Controller. Oil droplets of encapsulated single cells and barcoded beads (GEMs) were subsequently reverse transcribed in a Veriti Thermal Cycler, resulting in cDNA tagged with a cell barcode and unique molecular index (UMI). cDNA was amplified to generate single-cell libraries according to the manufacturer's protocol. Quantification was made with an Agilent Bioanalyzer High Sensitivity DNA assay (Agilent, High-Sensitivity DNA Kit, 5067–4626). Amplified cDNA was enzymatically fragmented, end-repaired, and poly-A tagged. Cleanup and size selection was performed on amplified cDNA using SPRIselect magnetic beads (Beckman-Coulter, SPRIselect, B23317). Next, Illumina sequencing adapters were ligated to the fragments and cleaned up using SPRIselect magnetic beads. Then, sample indices were selected and amplified, followed by a double-sided size selection using SPRIselect magnetic beads. We assessed the final library quality using an Agilent Bioanalyzer High Sensitivity DNA assay, and sequenced samples on Illumina NovaSeq 6000 as paired-end mode with 90 bp read2 and 20,000 reads depth. Four samples for detection of chromosomal alteration were sequenced with 270 bp read2 to achieve 80,000 reads per cell for gene expression.

Alignment, quantification, and quality control of scRNA-seq data

We processed droplet libraries using Cell Ranger 6.0.0 (10X Genomics). Sequencing reads were aligned with STAR[68] using the GRCh38 human reference genome. We created raw count matrices with the cellranger_count function. We processed them with the remove-background function of CellBender (v0.1.0)[52] to remove cell-free ambient RNAs in the droplets and call cells. We removed cells that had fewer than 1,000 UMIs or greater than 99th percentile of UMIs in each sample, fewer than 200 feature counts or greater than 99th percentile of feature counts in each sample, greater than 12% of reads from mitochondrial genes, or greater than 10% of reads from hemoglobin genes. We further excluded putative doublets using DoubletFinder (v2.0.3)[55] for each sample.

scRNA-seq computation pipelines

We used Seurat (v4.1.0)[33] for data scaling, transformation, clustering, dimensionality reduction differential expression analysis, and most visualization. We scaled and transformed data using the SCTransform() function, and linear regression was performed to remove unwanted variation due to the percentage of mitochondrial reads. We removed batch effects and integrated scRNA-seq datasets using Scanorama.[63] We performed a PC analysis based on adjusted gene expression and uniform manifold approximation and projection (UMAP) using the first 30 PCs. A nearest-neighbor graph using the first 30 PCs was calculated with the FindNeighbors() function, followed by clustering with the FindClusters() function setting the resolution parameter between 0.4 and 1.2.

We determined cellular identity with differentially expressed genes for each cluster using the FindMarkers() with parameter 'test.use = wilcox', and comparing those markers to known cell-type-specific genes. We temporally divided the whole PBMCs into four cell groups; T cells, natural killer (NK) cells, B cells, and monocytes (Mono)/dendritic cells (DC). We excluded platelets at this step. We reclustered each cell group in the same way as above and annotated cells using marker genes with reference to Azimuth.[33] First, we identified seven major cell types: CD4$^+$ T (CD4T) cells, CD8$^+$ T (CD8T) cells, other T (Other T) cells, NK cells, B cells, Mono, and DC. Then we divided them into 19 subsets: CD4$^+$ naive T (CD4 Naive) cells, CD4$^+$ memory T (CD4 Memory) cells, CD4$^+$ cytotoxic T (CD4 CTL) cells, regulatory T (Treg) cells, CD8$^+$ naive T (CD8 Naive) cells, CD8$^+$ memory T (CD8 Memory) cells, CD8$^+$ cytotoxic T (CD8 CTL) cells, mucosal-associated invariant T (MAIT) cells, gamma-delta T (gdT) cells, double-negative T (dnT) cells, CD56-dim natural killer (NK CD56^{dim}) cells, CD56-bright natural killer (NK CD56^{bright}) cells, Naive B (B Naive) cells, memory B (B Memory) cells, plasmablasts, CD14$^+$ monocytes (CD14 Mono), CD16$^+$ monocytes (CD16 Mono), conventional dendritic cells (cDC), and plasmacytoid dendritic cells (pDC).

Differential expression analysis using scRNA-seq data

Differential gene expression analysis was performed between patients with NMOSD and healthy controls in the *CCR6*-enriched cell types. We created donor pseudo-bulk samples by aggregating gene counts for each cell type within each sample. Genes which expression rate was more than 1% in each cell type were included in the analysis. Differential gene expression testing was performed using an NB GLM implemented in the Bioconductor package edgeR (v3.32.0).[56] We included age and sex in the model as covariates.

Single-cell eQTL analysis

First, we performed normalization of scRNA-seq datasets using scran (v1.18.5),[66] then calculated gene expression per cell type per sample as the mean of log$_2$-transformed counts-per-cell normalized expression. We adopted genes expressed in more than 1% of each cell type for PC analysis. We evaluated the dosage effect of the variant on the gene expression using linear regression models with the top two PCs of the genotype, the top two PCs of the gene expression, age, and gender as covariates. To correct multiple testing, FDR was calculated via the Benjamini-Hochberg method across all pairs of cell types and clinical status.

Cell-cell interaction analysis in PBMCs

At first, to reduce the influence of individual samples contributing a larger number of cells, we capped the number of cells per sample at 4,000 randomly sampled cells. We used the ComputeCommunProb() function in CellChat (v.2.1.0)[35] to calculate the weight of cell-cell interactions. We primarily set the parameter as type = "trimean", and switched to type = "truncatedMean" and trim = 0.01 when examining the interaction between *CCL20* and *CCR6*. After calculating interactions between 19 cell types, we extracted the cell types of interest and created the heatmaps.

Reference-based annotation of CD4T cells

We projected our CD4T cells dataset to reference atlas,[36] using the pipeline available at https://github.com/yyoshiaki/screfmapping. In this pipeline, FindTransferAnchors() function in Seurat is used to find anchors between the reference and query object, and TransferData() function is used to transfer information from the reference to the query. The pipeline was run with the default parameters. We annotated Th17 cells by combining Tcm (Th17) and Tem (Th1/17) in the reference data.

Differential abundance analysis

We used Milo (v1.2.0)[59] to test for the differential abundance of CD4T cells within defined neighborhoods between NMOSD and healthy controls. We first used the buildGraph() function to construct a KNN graph with parameters $k = 30$ and $d = 30$. Next we used makeNhoods() function to assign cells to neighborhoods based on their connectivity over the KNN graph. For computational efficiency, we subsampled 5% of all CD4T cells in this step. In testNhoods() function, we included age and sex as covariates. We did not apply a spatial FDR threshold to get a general estimate of the cell abundance. Log$_2$ FC of the number of cells between NMOSD and healthy controls in each neighborhood was used for visualization.

pQTL analysis

We measured expressions of 2,943 circulating proteins using Olink Explore 3072 platform from plasma of 1,394 independent East Asian individuals on the Japan COVID-19 Task Force (JCTF),[37–39] a nationwide multicenter consortium to overcome the COVID-19 pandemic in Japan. The expression levels in a normalized scale (Normalized Protein eXpression: NPX) were bridge-normalized using OlinkAnalyze R package and subsequently rank-inverse normal transformed.

We conducted a pQTL analysis using PLINK version 2.0[61] for the GWAS risk variant. We performed a linear regression analysis of genotypes for each circulating protein biomarker, adjusting for age, sex, top 4 genetic PCs, and top 6 expression PCs.

Associations between disease risks and mCAs

We evaluated the associations between mCAs and the risk of autoimmune diseases and hematological malignancy. From the GWAS control, we excluded hematological malignancy patients for this analysis ($n_{control}$ = 48,394). Using BBJ and our in-house data, we enrolled the patients with NMOSD (n = 232), MS (n = 599), RA (n = 2,789), SLE (n = 388), psoriasis vulgaris (n = 287), Sjögren's syndrome (n = 242), sarcoidosis (n = 79), and hematological malignancy (n = 1,301) after QC of the mCA detection. We applied the MoChA pipeline[11,12] to the genotype data from those samples. In brief, IDAT genotype intensity data were transformed to VCF files with $\log_2$ R ratio (LRR; total allelic intensity) and B-allele frequency (BAF; relative allelic intensity) values. Genotype phasing was performed in the same way as in the NMOSD GWAS. Using the phase information and LRR/BAF values, we detected individuals with mCAs including gain, loss, and CN-LOH. From the resulting candidates, calls flagged as germline copy number polymorphisms and calls that were likely germline duplications were removed. We additionally removed unclassifiable calls and calls with lower cell fraction (<0.01). We assessed the associations between each disease and CNA or CN-LOH using a multivariate logistic regression adjusted for age, age^2, and sex. We defined the recurrently affected regions as chromosomal regions (>10Mb) where more than one NMOSD patient shared mCAs.

Single-cell dissection of somatically mutated cells in NMOSD patients

We applied Numbat (v1.3.0)[35] to the additional scRNA-seq data of NMOSD patients with mCAs detected using the genotype data. Numbat combines population haplotype information with allele and expression signals from scRNA-seq data to enhance detection of somatic clones with mCAs. Utilizing the profiles of the genotype-based mCAs as prior information, we ran Numbat with parameters init_k = 10 and max_entropy = 1.0 and classified all the cells as somatically mutated cells or normal ones. For the TCR clonotype analysis using scVDJ-seq, filtered annotated contigs for TCR sequences were analyzed using Scirpy.[65] Among cells with both TCR α-chain and β-chain, TCR clonotypes were defined based on the similarity of CDR3 amino acid sequences with receptor_arms = "any", metric = "alignment", and default cutoff of ten. The DEG analysis between the 21q loss and normal CD4T cells were performed using a negative binomial model implemented in lme4 R library (v.1.1.32)[57] with an offset term for UMI count and random effects for sample. Genes were included if they were expressed in more than 10% of cells and were considered to be significant if they satisfied FDR (adjusted p-values via the Benjamini-Hochberg method) < 0.1. For the significant DEGs, the pathway enrichment analysis was performed using the enrichGO function of Clusterprofiler[53] with parameters OrgDb = "org.Hs.e.g.,.db" and ont = "BP". The statistical significance of the enrichment was adjusted via the Benjamini-Hochberg method.

QUANTIFICATION AND STATISTICAL ANALYSIS

Please refer to figure legends and method details for details of statistical analysis.